arXiv:1403.7457v1 [hep-ph] 28 Mar 2014

Heavy tetraquark states and quarkonium hybrids

Wei Chen* and T. G. Steele†
Department of Physics and Engineering Physics, University of Saskatchewan, Saskatoon, SK, S7N 5E2, Canada

Shi-Lin Zhu‡
Department of Physics and State Key Laboratory of Nuclear Physics and Technology, Peking University, Beijing 100871, China, and Collaborative Innovation Center of Quantum Matter, Beijing 100871, China

Many of the XYZ resonances observed by the Belle, Babar, CLEO and BESIII collaborations in the past decade are difficult to interpret as conventional quark-antiquark mesons, motivating the consideration of scenarios such as multi-quark states, meson molecules, and hybrids. After a brief introduction to QCD sum-rule methods, we provide a brief but comprehensive review of the mass spectra of the quarkonium-like tetraquark states $qQ\bar{q}\bar{Q}$, doubly charmed/bottomed tetraquark states $QQ\bar{q}\bar{q}$ and the heavy quarkonium hybrid states $\bar{Q}GQ$ in the QCD sum rules approach. Possible interpretations of the XYZ resonances are briefly discussed.

PACS numbers: 12.38.Lg, 11.40.-q, 12.39.Mk
Keywords: QCD sum rules, tetraquarks, hybrids

I. INTRODUCTION

In the conventional quark model (QM), hadrons, including the $q\bar{q}$ mesons and qqq baryons, are bound states of quarks and anti-quarks [1, 2]. The strong interaction of the colored quarks and gluons emerges from the low-energy regime of quantum chromodynamics (QCD), which is the most technically-challenging aspect of the standard model (SM). The hadron spectrum is therefore of great importance to our understanding of QCD.

In the quark model, a $q\bar{q}$ meson is a color-singlet state, which is composed of a quark color triplet and an antiquark color antitriplet. For a neutral $q\bar{q}$ state, its parity and charge conjugation parity are $P=(-)^{L+1}$ and $C=(-)^{L+S}$ respectively, where L is the relative momentum and S is the total spin. Thus the allowed J^{PC} quantum numbers for a neutral $q\bar{q}$ meson are $J^{PC}=0^{++},0^{-+},1^{++},1^{--},1^{+-},2^{++},2^{--},2^{-+},\cdots$. Most of the experimentally observed mesons can be interpreted as a conventional $q\bar{q}$ state. However, a $q\bar{q}$ pair can also be a color octet in QCD, which may combine with the other colored objects such as an excited gluonic field to form a hybrid meson ($\bar{q}gq$). Hybrid mesons are very interesting since they are allowed to carry not only the ordinary quantum numbers of the $q\bar{q}$ mesons listed above, but also exotic quantum numbers such as $J^{PC}=0^{--},0^{+-},1^{-+},2^{+-},\cdots$, which are not accessible to simple $q\bar{q}$ states. The study of the hybrid mesons provides an important platform to understand QCD as the theory of the strong interaction, including characteristics of color confinement.

Since the first investigation of hybrid mesons by Jaffe in 1976 [3], light hybrids were extensively studied in the MIT Bag model [4, 5], flux tube model [6–10], lattice QCD [11–14] and QCD sum rules [15–22]. To date, there has been some experimental evidence of the exotic light hybrid with $J^{PC}=1^{-+}$ [23–28]. For the heavy quarkonium hybrids, there are also many calculations performed in the constituent gluon model [29], the flux tube model [8], QCD sum rules [30–38], nonrelativistic QCD [39] and lattice QCD [40–45].

The diquark pair is another interesting color non-singlet bilinear operator in QCD. The color structure of a qq diquark can be symmetric $\mathbf{6_c}$ or antisymmetric $\bar{\mathbf{3}}_\mathbf{c}$ with similar flavor structure. Without inserting the covariant derivative, the spin and parity of a diquark operator can be determined by its color, flavor and Lorentz structures. The Lorentz structures are classified by using different kinds of γ matrices resulting in six distinct diquark operators in Lorentz space: $q_a^TCq_b$, $q_a^TC\gamma_5q_b$, $q_a^TC\gamma_\mu q_b$, $q_a^TC\gamma_\mu\gamma_5q_b$, $q_a^TC\sigma_{\mu\nu}q_b$, and $q_a^TC\sigma_{\mu\nu}\gamma_5q_b$, where a,b are the color indices. Since $q_a^TC\sigma_{\mu\nu}\gamma_5q_b$ and $q_a^TC\sigma_{\mu\nu}q_b$ carry opposite parity, we consider both operators although they overlap in the quantum numbers they can probe (see Table I). These six diquark operators are listed in Table I with their spins, parities, flavor, color and Lorentz structures, which are constrained by fermi statistics. As will be seen below, these operators play a very important role in the study of the tetraquark states.

*Electronic address: wec053@mail.usask.ca
†Electronic address: tom.steele@usask.ca
‡Electronic address: zhusl@pku.edu.cn

$q\Gamma q$	J^P	States	(Flavor, Color)
$q_a^T C\gamma_5 q_b$	0^+	$^1S_0$	$(\mathbf{6_f},\mathbf{6_c}),(\bar{\mathbf{3}}_\mathbf{f},\bar{\mathbf{3}}_\mathbf{c})$
$q_a^T C q_b$	0^-	$^3P_0$	$(\mathbf{6_f},\mathbf{6_c}),(\bar{\mathbf{3}}_\mathbf{f},\bar{\mathbf{3}}_\mathbf{c})$
$q_a^T C\gamma_\mu\gamma_5 q_b$	1^-	$^3P_1$	$(\mathbf{6_f},\mathbf{6_c}),(\bar{\mathbf{3}}_\mathbf{f},\bar{\mathbf{3}}_\mathbf{c})$
$q_a^T C\gamma_\mu q_b$	1^+	$^3S_1$	$(\mathbf{6_f},\bar{\mathbf{3}}_\mathbf{c}),(\bar{\mathbf{3}}_\mathbf{f},\mathbf{6_c})$
$q_a^T C\sigma_{\mu\nu} q_b$	$\begin{cases}1^-, & \text{for } \mu,\nu=1,2,3\\ 1^+, & \text{for } \mu=0,\nu=1,2,3\end{cases}$	$^1P_1$ $^3S_1$	$(\mathbf{6_f},\bar{\mathbf{3}}_\mathbf{c}),(\bar{\mathbf{3}}_\mathbf{f},\mathbf{6_c})$
$q_a^T C\sigma_{\mu\nu}\gamma_5 q_b$	$\begin{cases}1^+, & \text{for } \mu,\nu=1,2,3\\ 1^-, & \text{for } \mu=0,\nu=1,2,3\end{cases}$	$^3S_1$ $^1P_1$	$(\mathbf{6_f},\bar{\mathbf{3}}_\mathbf{c}),(\bar{\mathbf{3}}_\mathbf{f},\mathbf{6_c})$

TABLE I: Properties of the diquark operators.

Tetraquarks ($qq\bar{q}\bar{q}$) are composed of diquarks and antidiquarks. They are bound by the color force between quarks. The tetraquarks are generally unstable because they can decay easily into two mesons through kinematically-allowed fall-apart mechanisms and thus they are expected to be very broad resonances. The low-lying scalar mesons below 1 GeV have been considered as good candidates of the light tetraquark states [46, 47]. In the heavy quark sector, some of the recently observed quarkoniumlike states were suggested to be candidates for hidden charm/bottom $Q\bar{Q}q\bar{q}$-type tetraquark states [48–53], where Q denotes a heavy quark (bottom or charm) and q denotes a light quark (up, down, strange).

Another possibility for heavy tetraquarks are the doubly charmed/bottomed $QQ\bar{q}\bar{q}$-type states. This color-singlet four-quark configuration is also allowed in QCD. When the heavy quark QQ pair is spatially close, it would act as a pointlike antiheavy quark color source $\bar{Q}$ and pick up two light antiquarks $\bar{q}\bar{q}$ to form the bound state $QQ\bar{q}\bar{q}$. Such a doubly charmed/bottomed tetraquark system is the QCD analogue of the hydrogen molecule in QED, in which two electrons are shared by two protons. The existence and stability of the doubly charmed/bottomed tetraquark systems have been studied in many different models, such as the MIT bag model [54], QCD sum rules [55–58], chiral quark model [59, 60], constituent quark model [61–65], chiral perturbation theory [66] and some other methods [67–75].

In the past decade many unexpected mesons, the so called XYZ states, were discovered at B-factories. These states contain a heavy quark-antiquark pair and are above the open-charm/bottom threshold. To date, there are 15 neutral and 5 charged states in the charmonium sector while one neutral and two charged states in the bottomonium sector [76]. Some of these states are surprisingly narrow. Some are even charged. Many of these states do not fit in the conventional quark model and are considered as candidates for exotic states. The underlying structure of these newly observed XYZ states inspired the extensive study of the hadron spectrum. Many theoretical speculations have been proposed to interpret these new resonances, such as molecular states, quarkoniumlike tetraquark states, quarkonium hybrids and conventional quarkonium states. To understand the nature of these XYZ states, further theoretical investigations of the exotic hadron spectrum are still needed.

We organize this review as follows. In Sec. II, we briefly introduce the general procedure of QCD sum rules, including the two-point correlation functions, the operator product expansion, the Borel transform, quark-hadron duality and the mass sum rules. In Sec. III, we give the interpolating currents of the quarkoniumlike tetraquark systems, the doubly charmed/bottomonium tetraquark systems and the quarkonium hybrid systems. The correlation functions and spectral densities are calculated using these currents. We perform QCD sum rule analysis of all three hadron systems and extract the masses of the lowest lying states. In the last section we summarize our results and comment on their implications for heavy quarkonium spectroscopy.

II. QCD SUM RULES

QCD sum rules provide a very powerful nonperturbative method for studying hadron structures [77–80]. IN addition to the operator product expansion, a key idea of the method is quark-hadron duality: the equivalence of (integrated) correlation functions at both the hadronic level and the quark-gluonic level.

A. Two-point correlation function

In general, the two-point correlation function for a scalar or pseudoscalar operator is defined as

$$\Pi(q) = i \int d^4x e^{iq\cdot x} \langle 0|T[J(x)J^\dagger(0)]|0\rangle, \tag{1}$$

where $J(x)$ is an interpolating current that can couple to a scalar or pseudoscalar resonance and T denotes the time-ordered product. For a vector or axial-vector interpolating current $J_\mu(x)$, the corresponding two-point correlation function reads

$$\begin{aligned}\Pi_{\mu\nu}(q) &= i \int d^4x e^{iq\cdot x} \langle 0|T[J_\mu(x)J_\nu^\dagger(0)]|0\rangle \\ &= \eta_{\mu\nu}\Pi_1(q^2) + \frac{q_\mu q_\nu}{q^2}\Pi_0(q^2),\end{aligned} \tag{2}$$

in which $\eta_{\mu\nu} = q_\mu q_\nu/q^2 - g_{\mu\nu}$ is the tensor structure of the spin-1 invariant function $\Pi_1(q^2)$. The spin-0 invariant function $\Pi_0(q^2)$ also appears in Eq. (2) when $J_\mu(x)$ is not a conserved vector current. We will introduce the choice of the interpolating currents that couple to the heavy tetraquarks and quarkonium hybrids in the next section.

At the hadronic level, the invariant function $\Pi(q^2)$ can be expressed in the form of the dispersion relation with its imaginary part

$$\Pi(q^2) = \frac{(q^2)^N}{\pi} \int \frac{\mathrm{Im}\Pi(s)}{s^N(s - q^2 - i\epsilon)} ds + \sum_{n=0}^{N-1} b_n (q^2)^n, \tag{3}$$

in which b_n are the N unknown subtraction constants which can be removed by taking the Borel transform. With a narrow resonance approximation, the imaginary part of the correlation function is obtained by inserting intermediate states $|n\rangle$ for the hadron we want to study. The imaginary part can be written as a sum over δ functions,

$$\mathrm{Im}\Pi(s) = \pi \sum_n \delta(s - m_n^2) \langle 0|J|n\rangle\langle n|J^\dagger|0\rangle, \tag{4}$$

in which the intermediate states $|n\rangle$ carry the same quantum numbers as the interpolating current $J(x)$. The correlation function $\Pi(q^2)$ contains the contributions from all resonances that can couple to $J(x)$, including the lowest lying ground state and the excited higher states. In QCD sum rules, one usually parametrizes the spectral function $\rho(s)$ with a pole plus continuum approximation,

$$\rho(s) = \frac{1}{\pi}\mathrm{Im}\Pi(s) = f_X^2 \delta(s - m_X^2) + \text{continuum}, \tag{5}$$

where m_X is the mass of the lowest lying resonance $|X\rangle$ and f_X is the coupling parameter of the current $J(x)$ with $|X\rangle$. For a scalar or pseudoscalar current $J(x)$ and vector or axial-vector current $J_\mu(x)$, we have

$$\langle 0|J|X\rangle = f_X, \tag{6}$$

$$\langle 0|J_\mu|X\rangle = f_X \epsilon_\mu, \tag{7}$$

where ϵ_μ is the polarization vector ($\epsilon \cdot q = 0$).

B. Operator product expansion

The two-point correlation function can also be calculated at the quark-gluonic level via the operator product expansion (OPE) [81]:

$$\Pi(q) = i \int d^4x e^{iq\cdot x} \langle 0|T[J(x)J^\dagger(0)]|0\rangle = \sum_n C_n(Q^2) O_n\,,\ Q^2 = -q^2\,, \tag{8}$$

where $C_n(Q^2)$ are the Wilson coefficients and O_n are the vacuum expectation values of the local gauge invariant operators constructed from the quark and gluon fields. The Wilson coefficients $C_n(Q^2)$ can be calculated in perturbation theory and expressed in terms of the QCD parameters such as the quark mass and the strong coupling constant α_s.

The long distance nonperturbative effects are included in the various condensates O_n, which are ordered by increasing dimension in the expansion. Except for the unit operator I, the QCD vacuum condensates up to dimension-eight include: the quark condensate $\langle\bar{q}q\rangle$, gluon condensate $\langle g_s^2GG\rangle$, quark-gluon mixed condensate $\langle\bar{q}g_s\sigma\cdot Gq\rangle$, tri-gluon condensate $\langle g_s^3fGGG\rangle$, four quark condensate $\langle\bar{q}q\rangle^2$, and condensate $\langle\bar{q}q\rangle\langle\bar{q}g_s\sigma\cdot Gq\rangle$.

To calculate the correlation function $\Pi(q)$, we need the full quark propagator including quark and gluon condensates [78, 82]

$$\begin{aligned} iS_q^{ab}(x) &= \frac{i\delta^{ab}}{2\pi^2x^4}\hat{x} + \frac{i}{32\pi^2}\frac{\lambda_{ab}^n}{2}g_sG_{\mu\nu}^n\frac{1}{x^2}(\sigma^{\mu\nu}\hat{x}+\hat{x}\sigma^{\mu\nu}) - \frac{\delta^{ab}}{12}\langle\bar{q}q\rangle + \frac{\delta^{ab}x^2}{192}\langle\bar{q}Gq\rangle - \frac{m_q\delta^{ab}}{4\pi^2x^2} \\ &\quad + \frac{i\delta^{ab}m_q\langle\bar{q}q\rangle}{48}\hat{x} - \frac{im_q\langle\bar{q}Gq\rangle\delta^{ab}x^2\hat{x}}{1152}, \end{aligned} \tag{9}$$

$$iS_Q^{ab}(p) = \frac{i\delta^{ab}}{\hat{p}-m_Q} + \frac{i}{4}g_s\frac{\lambda_{ab}^n}{2}G_{\mu\nu}^n\frac{\sigma^{\mu\nu}(\hat{p}+m_Q)+(\hat{p}+m_Q)\sigma^{\mu\nu}}{(p^2-m_Q^2)^2} + \frac{i\delta^{ab}}{12}\langle g_s^2GG\rangle m_Q\frac{p^2+m_Q\hat{p}}{(p^2-m_Q^2)^4}, \tag{10}$$

in which q represents u, d or s quarks and Q represents c or b quarks. The superscripts a, b are the color indices and $\hat{x}=\gamma_\mu x^\mu$, $\hat{p}=\gamma_\mu p^\mu$. One notes that for the light quarks, we use the propagator in coordinate space. For heavy quarks, the momentum space expression is sometimes more convenient.

C. Mass sum rules

The fundamental assumption in the QCD sum rules is quark-hadron duality, which matches the two descriptions of the correlation function at both the hadronic level and quark-gluon level. To pick out the lowest lying resonance of interest, one defines the Borel transform,

$$B\left[\Pi(q^2)\right] = \lim_{\substack{-q^2,n\to\infty \\ -q^2/n\equiv M_B^2}} \frac{1}{n!}(-q^2)^{n+1}\left(\frac{d}{dq^2}\right)^n\Pi(q^2), \tag{11}$$

where the Borel mass $M_B^2\equiv -q^2/n$ is introduced instead of q^2. Performing the Borel transform of the dispersion relation in Eq. (3), we can remove the unknown subtraction terms and suppress the contributions from the excited states and continuum. On the OPE side, the Borel transform can improve the convergence of the OPE series by suppressing the contribution from the high dimension condensates.

To establish the mass sum rules, we perform the Borel transform of the correlation function $\Pi(q^2)$ obtained at both levels

$$f_X^2m_X^{2k}e^{-m_X^2/M_B^2} = \int_{4m_Q^2}^{s_0} ds e^{-s/M_B^2}\rho(s)s^k = \mathcal{L}_k\left(s_0, M_B^2\right), \tag{12}$$

where s_0 is the continuum threshold. On the left hand of Eq. (12), we have used the spectral function defined in Eq. (5). The lowest lying hadron mass is then extracted as,

$$m_X\left(s_0, M_B^2\right) = \sqrt{\frac{\mathcal{L}_1\left(s_0, M_B^2\right)}{\mathcal{L}_0\left(s_0, M_B^2\right)}}. \tag{13}$$

The continuum threshold s_0 and Borel mass M_B are the two most important parameters in a QCD sum rule analysis. The stability of QCD sum rules requires a suitable working region. To obtain the Borel window, one should study the OPE convergence and the pole contribution. The criterion of OPE convergence determines a lower bound on M_B^2 while the constraint of the pole contribution leads to its upper bound. The pole contribution (PC) is defined as

$$\mathrm{PC}(s_0, M_B^2) = \frac{\mathcal{L}_0\left(s_0, M_B^2\right)}{\mathcal{L}_0\left(\infty, M_B^2\right)}, \tag{14}$$

which is a function of s_0 and M_B. This definition comes from the sum rules established in Eq. (12) and indicates the contribution of the lowest lying resonance to the correlation function. For the continuum threshold s_0, an optimized choice is the value minimizing the variation of the extracted hadron mass m_X with the Borel mass M_B^2.

D. Input parameters

So far, we have introduced the sum rules in Eq. (12) and extracted the mass of the lowest lying ground hadron state in Eq. (13). They are expressed as functions of the quark masses, strong coupling α_s, various QCD condensates, continuum threshold s_0 and Borel mass M_B. To perform a numerical analysis, we adopt the following values of these parameters: [2, 78, 83–86]:

$$\begin{aligned}
&m_q = m_u = m_d = 0,\\
&m_s(2\,\text{GeV}) = (101^{+29}_{-21})\ \text{MeV}\,,\\
&m_c(\mu = m_c) = \overline{m}_c = (1.23 \pm 0.09)\ \text{GeV}\,,\\
&m_b(\mu = m_b) = \overline{m}_b = (4.20 \pm 0.07)\ \text{GeV}\,,\\
&\langle\bar{q}q\rangle = -(0.23 \pm 0.03)^3\ \text{GeV}^3\,,\\
&\langle\bar{q}g_s\sigma\cdot Gq\rangle = -M_0^2\langle\bar{q}q\rangle\,,\\
&M_0^2 = (0.8 \pm 0.2)\ \text{GeV}^2\,,\\
&\langle\bar{s}s\rangle/\langle\bar{q}q\rangle = 0.8 \pm 0.2\,,\\
&\langle g_s^2GG\rangle = (0.48 - 0.94)\text{GeV}^4\,,\\
&\langle g_s^3fGGG\rangle = -(8.2 \pm 1.0)\ \text{GeV}^2\langle\alpha_sGG\rangle,\\
&\langle g_s^4jj\rangle = -\frac{4}{3}g_s^4\langle\bar{q}q\rangle^2,
\end{aligned} \tag{15}$$

in which we keep $m_u = m_d = 0$ in the chiral limit. The charm and bottom quark masses are the running masses in the $\overline{\text{MS}}$ scheme. One should be very cautious about the extra minus sign in the values $\langle\bar{q}g_s\sigma\cdot Gq\rangle$ and $\langle g_s^3fGGG\rangle$, which comes from our convention for the covariant derivative and strong coupling constant g_s.

For the conventional meson sum rules, the quark condensate $\langle\bar{q}q\rangle$ and gluon condensate $\langle g_s^2GG\rangle$ are the dominant nonperturbative contributions to the correlation functions and the contributions of the higher dimension condensates are usually suppressed. However, the situations are different for the exotic hadrons, such as the molecular and tetraquark states. In these systems, the quark-gluon mixed condensate $\langle\bar{q}g_s\sigma\cdot Gq\rangle$, four-quark condensate $\langle\bar{q}q\bar{q}q\rangle$, and even the dimension-8 condensate $\langle\bar{q}q\bar{q}g_s\sigma\cdot Gq\rangle$ will play very important roles. The values of the four-quark condensate and the dimension-8 condensate are estimated using the vacuum factorization assumption [87, 88]

$$\langle\bar{q}q\bar{q}q\rangle \sim \langle\bar{q}q\rangle^2, \langle\bar{q}q\bar{q}g_s\sigma\cdot Gq\rangle \sim \langle\bar{q}q\rangle\langle\bar{q}g_s\sigma\cdot Gq\rangle. \tag{16}$$

For the hybrid charmonium and bottomonium analyses, the correlation functions and the spectral densities are evaluated up to dimension six tri-gluon condensate $\langle g_s^3fGGG\rangle$ at the leading order of α_s. The tri-gluon condensate $\langle g_s^3fGGG\rangle$ was found to stabilize the mass sum rules in these systems [34–38]. The strong coupling is then determined at the scale μ appropriate to the system by the evolution from the τ and Z masses, respectively:

$$\alpha_s(\mu) = \frac{\alpha_s(M_\tau)}{1+\frac{25\alpha_s(M_\tau)}{12\pi}\log(\frac{\mu^2}{M_\tau^2})}, \quad \alpha_s(M_\tau) = 0.33; \tag{17}$$

$$\alpha_s(\mu) = \frac{\alpha_s(M_Z)}{1+\frac{23\alpha_s(M_Z)}{12\pi}\log(\frac{\mu^2}{M_Z^2})}, \quad \alpha_s(M_Z) = 0.118, \tag{18}$$

in which the τ and Z masses, $\alpha_s(M_\tau)$ and $\alpha_s(M_Z)$ are from the Particle Data Group [2].

III. CONSTRUCTION OF THE INTERPOLATING CURRENTS

In general, there are two types of constructions of the four-quark interpolating currents: tetraquark-type $(qq)(\bar{q}\bar{q})$ and molecular-type $(\bar{q}q)(\bar{q}q)$. However, these two constructions are equivalent by using Fierz transformations [89, 90]. In this section, we construct all heavy tetraquark-type $(qQ)(\bar{q}\bar{Q})$ and $(QQ)(\bar{q}\bar{q})$ interpolating currents. These currents have definite quantum numbers, flavor and color structures. We will also introduce the quarkonium hybrid interpolating currents with various quantum numbers.

A. Hidden charm/bottom tetraquark $Qq\bar{Q}\bar{q}$ interpolating currents

To construct the diquark-antidiquark type of tetraquark currents, we consider the six diquark fields and the corresponding antidiquark fields as introduced in Table I and compose a six-order matrix O. The elements of O are the tetraquark operators, which are composed by multiplying a diquark and an antidiquark pair. The spins and parities of the matrix elements with $J \leq 1$ are listed in Table II.

Operators		$\bar{q}_a\gamma_5 C\bar{Q}_b^T$	$\bar{q}_a C\bar{Q}_b^T$	$\bar{q}_a\gamma_\mu\gamma_5 C\bar{Q}_b^T$	$\bar{q}_a\gamma_\mu C\bar{Q}_b^T$	$\bar{q}_a\sigma_{\mu\nu} C\bar{Q}_b^T$	$\bar{q}_a\sigma_{\mu\nu}\gamma_5 C\bar{Q}_b^T$
	J^P	0^+	0^-	1^-	1^+	1^-	1^+
$q_a^T C\gamma_5 Q_b$	0^+	0^+	0^-	1^-	1^+	$-$	$-$
$q_a^T C Q_b$	0^-	0^-	0^+	1^+	1^-	$-$	$-$
$q_a^T C\gamma_\mu\gamma_5 Q_b$	1^-	1^-	1^+	0^+	0^-	1^+	1^-
$q_a^T C\gamma_\mu Q_b$	1^+	1^+	1^-	0^-	0^+	1^-	1^+
$q_a^T C\sigma_{\mu\nu} Q_b$	1^-	$-$	$-$	1^+	1^-	0^+	0^-
$q_a^T C\sigma_{\mu\nu}\gamma_5 Q_b$	1^+	$-$	$-$	1^-	1^+	$-$	$-$

TABLE II: The spins and parities of the elements of the matrix O.

For this operator matrix O, its charge-conjugation partner equals to the transpose matrix O^T,

$$\mathbb{C}O_{ij}\mathbb{C}^{-1} = O_{ji}. \tag{19}$$

One notes that the operator O_{66} is equivalent to O_{55} while O_{65} is equivalent to O_{56}, including their spins and parities. Thus we do not use O_{66} and O_{65} in the construction of the currents. To compose a color singlet tetraquark current, the color structure of the tetraquark is either $\mathbf{6}\otimes\bar{\mathbf{6}}$ or $\bar{\mathbf{3}}\otimes\mathbf{3}$, which is denoted by $\mathbf{6}$ and $\mathbf{3}$ respectively. With the relation in Eq. (19), we can define the symmetric matrix S and antisymmetric matrix A,

$$S_{\mathbf{6}} = O_{\mathbf{6}} + O_{\mathbf{6}}^T, S_{\mathbf{3}} = O_{\mathbf{3}} + O_{\mathbf{3}}^T, \tag{20}$$
$$A_{\mathbf{6}} = O_{\mathbf{6}} - O_{\mathbf{6}}^T, A_{\mathbf{3}} = O_{\mathbf{3}} - O_{\mathbf{3}}^T, \tag{21}$$

in which $S_{\mathbf{6}}, A_{\mathbf{6}}$ have symmetric color structures and $S_{\mathbf{3}}, A_{\mathbf{3}}$ have antisymmetric color structures. It is easy to check that the tetraquark elements of S have even C-parities and the elements of A have odd C-parities. $A_{ii} = 0$ indicates that the $J^{PC} = 0^{+-}$ tetraquark currents without derivatives do not exist [90]. However, one can construct the tetraquark currents with such quantum numbers by using a covariant derivative [53].

Finally, we can obtain the tetraquark interpolating currents with $J^{PC} = 0^{-+}, 0^{--}, 1^{-+}, 1^{--}, 1^{++}$ and 1^{+-} from the matrices $S_{\mathbf{6}}, A_{\mathbf{6}}$, $S_{\mathbf{3}}$ and $A_{\mathbf{3}}$:

- The interpolating currents with $J^{PC} = 0^{-+}$ and 0^{--} are:

$$\begin{aligned}
J_1 &= S_{21}^{\mathbf{6}}(A_{21}^{\mathbf{6}}) = q_a^T CQ_b(\bar{q}_a\gamma_5 C\bar{Q}_b^T + \bar{q}_b\gamma_5 C\bar{Q}_a^T) \pm q_a^T C\gamma_5 Q_b(\bar{q}_a C\bar{Q}_b^T + \bar{q}_b C\bar{Q}_a^T)\,,\\
J_2 &= O_{56}^{\mathbf{3}} = q_a^T C\sigma_{\mu\nu} Q_b(\bar{q}_a\sigma^{\mu\nu}\gamma_5 C\bar{Q}_b^T - \bar{q}_b\sigma^{\mu\nu}\gamma_5 C\bar{Q}_a^T)\,,\\
J_3 &= S_{43}^{\mathbf{6}}(A_{43}^{\mathbf{6}}) = q_a^T C\gamma_\mu Q_b(\bar{q}_a\gamma^\mu\gamma_5 C\bar{Q}_b^T + \bar{q}_b\gamma^\mu\gamma_5 C\bar{Q}_a^T) \pm q_a^T C\gamma_\mu\gamma_5 Q_b(\bar{q}_a\gamma^\mu C\bar{Q}_b^T + \bar{q}_b\gamma^\mu C\bar{Q}_a^T)\,,\\
J_4 &= S_{43}^{\mathbf{3}}(A_{43}^{\mathbf{3}}) = q_a^T C\gamma_\mu Q_b(\bar{q}_a\gamma^\mu\gamma_5 C\bar{Q}_b^T - \bar{q}_b\gamma^\mu\gamma_5 C\bar{Q}_a^T) \pm q_a^T C\gamma_\mu\gamma_5 Q_b(\bar{q}_a\gamma^\mu C\bar{Q}_b^T - \bar{q}_b\gamma^\mu C\bar{Q}_a^T)\,,\\
J_5 &= S_{21}^{\mathbf{3}}(A_{21}^{\mathbf{3}}) = q_a^T CQ_b(\bar{q}_a\gamma_5 C\bar{Q}_b^T - \bar{q}_b\gamma_5 C\bar{Q}_a^T) \pm q_a^T C\gamma_5 Q_b(\bar{q}_a C\bar{Q}_b^T - \bar{q}_b C\bar{Q}_a^T)\,,\\
J_6 &= O_{56}^{\mathbf{6}} = q_a^T C\sigma_{\mu\nu} Q_b(\bar{q}_a\sigma^{\mu\nu}\gamma_5 C\bar{Q}_b^T + \bar{q}_b\sigma^{\mu\nu}\gamma_5 C\bar{Q}_a^T)\,,
\end{aligned} \tag{22}$$

  where "S" and "+" in J_1, J_3, J_4, J_5 correspond to $J^{PC} = 0^{-+}$, "A" and "$-$" correspond to $J^{PC} = 0^{--}$. J_2, J_6 couple to the states with $J^{PC} = 0^{-+}$.

- The interpolating currents with $J^{PC}=1^{-+}$ and 1^{--} are:

$$\begin{aligned}
J_{1\mu} &= S^{\mathbf{6}}_{13}(A^{\mathbf{6}}_{13}) = q_a^T C\gamma_5 Q_b(\bar{q}_a\gamma_\mu\gamma_5 C\bar{Q}_b^T + \bar{q}_b\gamma_\mu\gamma_5 C\bar{Q}_a^T) \pm q_a^T C\gamma_\mu\gamma_5 Q_b(\bar{q}_a\gamma_5 C\bar{Q}_b^T + \bar{q}_b\gamma_5 C\bar{Q}_a^T)\,,\\
J_{2\mu} &= S^{\mathbf{3}}_{45}(A^{\mathbf{3}}_{45}) = q_a^T C\gamma^\nu Q_b(\bar{q}_a\sigma_{\mu\nu} C\bar{Q}_b^T - \bar{q}_b\sigma_{\mu\nu} C\bar{Q}_a^T) \pm q_a^T C\sigma_{\mu\nu} Q_b(\bar{q}_a\gamma^\nu C\bar{Q}_b^T - \bar{q}_b\gamma^\nu C\bar{Q}_a^T)\,,\\
J_{3\mu} &= S^{\mathbf{3}}_{13}(A^{\mathbf{3}}_{13}) = q_a^T C\gamma_5 Q_b(\bar{q}_a\gamma_\mu\gamma_5 C\bar{Q}_b^T - \bar{q}_b\gamma_\mu\gamma_5 C\bar{Q}_a^T) \pm q_a^T C\gamma_\mu\gamma_5 Q_b(\bar{q}_a\gamma_5 C\bar{Q}_b^T - \bar{q}_b\gamma_5 C\bar{Q}_a^T)\,,\\
J_{4\mu} &= S^{\mathbf{6}}_{45}(A^{\mathbf{6}}_{45}) = q_a^T C\gamma^\nu Q_b(\bar{q}_a\sigma_{\mu\nu} C\bar{Q}_b^T + \bar{q}_b\sigma_{\mu\nu} C\bar{Q}_a^T) \pm q_a^T C\sigma_{\mu\nu} Q_b(\bar{q}_a\gamma^\nu C\bar{Q}_b^T + \bar{q}_b\gamma^\nu C\bar{Q}_a^T)\,,\\
J_{5\mu} &= S^{\mathbf{6}}_{24}(A^{\mathbf{6}}_{24}) = q_a^T C Q_b(\bar{q}_a\gamma_\mu C\bar{Q}_b^T + \bar{q}_b\gamma_\mu C\bar{Q}_a^T) \pm q_a^T C\gamma_\mu Q_b(\bar{q}_a C\bar{Q}_b^T + \bar{q}_b C\bar{Q}_a^T)\,,\\
J_{6\mu} &= S^{\mathbf{6}}_{36}(A^{\mathbf{6}}_{36}) = q_a^T C\gamma^\nu\gamma_5 Q_b(\bar{q}_a\sigma_{\mu\nu}\gamma_5 C\bar{Q}_b^T + \bar{q}_b\sigma_{\mu\nu}\gamma_5 C\bar{Q}_a^T) \pm q_a^T C\sigma_{\mu\nu}\gamma_5 Q_b(\bar{q}_a\gamma^\nu\gamma_5 C\bar{Q}_b^T + \bar{q}_b\gamma^\nu\gamma_5 C\bar{Q}_a^T)\,,\\
J_{7\mu} &= S^{\mathbf{3}}_{24}(A^{\mathbf{3}}_{24}) = q_a^T C Q_b(\bar{q}_a\gamma_\mu C\bar{Q}_b^T - \bar{q}_b\gamma_\mu C\bar{Q}_a^T) \pm q_a^T C\gamma_\mu Q_b(\bar{q}_a C\bar{Q}_b^T - \bar{q}_b C\bar{Q}_a^T)\,,\\
J_{8\mu} &= S^{\mathbf{3}}_{36}(A^{\mathbf{3}}_{36}) = q_a^T C\gamma^\nu\gamma_5 Q_b(\bar{q}_a\sigma_{\mu\nu}\gamma_5 C\bar{Q}_b^T - \bar{q}_b\sigma_{\mu\nu}\gamma_5 C\bar{Q}_a^T) \pm q_a^T C\sigma_{\mu\nu}\gamma_5 Q_b(\bar{q}_a\gamma^\nu\gamma_5 C\bar{Q}_b^T - \bar{q}_b\gamma^\nu\gamma_5 C\bar{Q}_a^T) \qquad (23)
\end{aligned}$$

  where "S" and "+" correspond to $J^{PC}=1^{-+}$, "A" and "$-$" correspond to $J^{PC}=1^{--}$.

- The interpolating currents with $J^{PC}=1^{++}$ and 1^{+-} are:

$$\begin{aligned}
J_{1\mu} &= S^{\mathbf{6}}_{23}(A^{\mathbf{6}}_{23}) = q_a^T C Q_b(\bar{q}_a\gamma_\mu\gamma_5 C\bar{Q}_b^T + \bar{q}_b\gamma_\mu\gamma_5 C\bar{Q}_a^T) \pm q_a^T C\gamma_\mu\gamma_5 Q_b(\bar{q}_a C\bar{Q}_b^T + \bar{q}_b C\bar{Q}_a^T)\,,\\
J_{2\mu} &= S^{\mathbf{3}}_{23}(A^{\mathbf{3}}_{23}) = q_a^T C Q_b(\bar{q}_a\gamma_\mu\gamma_5 C\bar{Q}_b^T - \bar{q}_b\gamma_\mu\gamma_5 C\bar{Q}_a^T) \pm q_a^T C\gamma_\mu\gamma_5 Q_b(\bar{q}_a C\bar{Q}_b^T - \bar{q}_b C\bar{Q}_a^T)\,,\\
J_{3\mu} &= S^{\mathbf{6}}_{14}(A^{\mathbf{6}}_{14}) = q_a^T C\gamma_5 Q_b(\bar{q}_a\gamma_\mu C\bar{Q}_b^T + \bar{q}_b\gamma_\mu C\bar{Q}_a^T) \pm q_a^T C\gamma_\mu Q_b(\bar{q}_a\gamma_5 C\bar{Q}_b^T + \bar{q}_b\gamma_5 C\bar{Q}_a^T)\,,\\
J_{4\mu} &= S^{\mathbf{3}}_{14}(A^{\mathbf{3}}_{14}) = q_a^T C\gamma_5 Q_b(\bar{q}_a\gamma_\mu C\bar{Q}_b^T - \bar{q}_b\gamma_\mu C\bar{Q}_a^T) \pm q_a^T C\gamma_\mu Q_b(\bar{q}_a\gamma_5 C\bar{Q}_b^T - \bar{q}_b\gamma_5 C\bar{Q}_a^T)\,,\\
J_{5\mu} &= S^{\mathbf{6}}_{46}(A^{\mathbf{6}}_{46}) = q_a^T C\gamma^\nu Q_b(\bar{q}_a\sigma_{\mu\nu}\gamma_5 C\bar{Q}_b^T + \bar{q}_b\sigma_{\mu\nu}\gamma_5 C\bar{Q}_a^T) \pm q_a^T C\sigma_{\mu\nu}\gamma_5 Q_b(\bar{q}_a\gamma^\nu C\bar{Q}_b^T + \bar{q}_b\gamma^\nu C\bar{Q}_a^T)\,,\\
J_{6\mu} &= S^{\mathbf{3}}_{46}(A^{\mathbf{3}}_{46}) = q_a^T C\gamma^\nu Q_b(\bar{q}_a\sigma_{\mu\nu}\gamma_5 C\bar{Q}_b^T - \bar{q}_b\sigma_{\mu\nu}\gamma_5 C\bar{Q}_a^T) \pm q_a^T C\sigma_{\mu\nu}\gamma_5 Q_b(\bar{q}_a\gamma^\nu C\bar{Q}_b^T - \bar{q}_b\gamma^\nu C\bar{Q}_a^T)\,,\\
J_{7\mu} &= S^{\mathbf{6}}_{35}(A^{\mathbf{6}}_{35}) = q_a^T C\gamma^\nu\gamma_5 Q_b(\bar{q}_a\sigma_{\mu\nu} C\bar{Q}_b^T + \bar{q}_b\sigma_{\mu\nu} C\bar{Q}_a^T) \pm q_a^T C\sigma_{\mu\nu} Q_b(\bar{q}_a\gamma^\nu\gamma_5 C\bar{Q}_b^T + \bar{q}_b\gamma^\nu\gamma_5 C\bar{Q}_a^T)\,,\\
J_{8\mu} &= S^{\mathbf{3}}_{35}(A^{\mathbf{3}}_{35}) = q_a^T C\gamma^\nu\gamma_5 Q_b(\bar{q}_a\sigma_{\mu\nu} C\bar{Q}_b^T - \bar{q}_b\sigma_{\mu\nu} C\bar{Q}_a^T) \pm q_a^T C\sigma_{\mu\nu} Q_b(\bar{q}_a\gamma^\nu\gamma_5 C\bar{Q}_b^T - \bar{q}_b\gamma^\nu\gamma_5 C\bar{Q}_a^T)\,, \qquad (24)
\end{aligned}$$

  where "S" and "+" correspond to $J^{PC}=1^{++}$, "A" and "$-$" correspond to $J^{PC}=1^{+-}$.

All the currents in Eqs. (22)–(24) should contain both the $uc\bar{u}\bar{c}$ and $dc\bar{d}\bar{c}$ parts to have the definite isospin and G-parity. However, we do not differentiate the up and down quarks in our analysis due to the $SU(2)$ flavor symmetry and denote them by q. Using these currents, we calculate the correlation functions and the spectral densities up to dimension eight. One can find the results of the spectral densities in Refs. [51, 52]. From these expressions, the nonperturbative terms include the quark condensate $\langle\bar{q}q\rangle$, quark-gluon mixed condensate $\langle\bar{q}g_s\sigma\cdot Gq\rangle$, gluon condensate $\langle g_s^2GG\rangle$, four-quark condensate $\langle\bar{q}q\rangle^2$ and dimension-8 condensate $\langle\bar{q}q\rangle\langle\bar{q}g_s\sigma\cdot Gq\rangle$. The tri-gluon condensate $\langle g_s^3fGGG\rangle$ is heavily suppressed in the heavy tetraquark systems and can be neglected [52]. To study the $sQ\bar{s}\bar{Q}$ systems, we keep the m_s dependent terms in the spectral densities.

B. Doubly charmed/bottomed tetraquark $QQ\bar{q}\bar{q}$ interpolating currents

For the $QQ\bar{q}\bar{q}$ systems, the heavy quark pair QQ has the symmetric flavor structure $\mathbf{6_f}$. According to Table I, its color structure is determined at the same time. To compose a color singlet tetraquark operator, the heavy quark pair should be multiplied by a light antiquark pair $\bar{q}\bar{q}$ with the same color structure. Considering the Pauli principle, we can obtain the following $QQ\bar{q}\bar{q}$ currents with $J^P=0^-, 0^+, 1^-$ and 1^+:

- For the currents with $J^P=0^-$,

$$\begin{aligned}
\eta_1 &= Q_a^T C Q_b(\bar{q}_a\gamma_5 C\bar{q}_b^T + \bar{q}_b\gamma_5 C\bar{q}_a^T),\\
\eta_2 &= Q_a^T C\gamma_5 Q_b(\bar{q}_a C\bar{q}_b^T + \bar{q}_b C\bar{q}_a^T),\\
\eta_3 &= Q_a^T C\sigma_{\mu\nu} Q_b(\bar{q}_a\sigma^{\mu\nu}\gamma_5 C\bar{q}_b^T - \bar{q}_b\sigma^{\mu\nu}\gamma_5 C\bar{q}_a^T),\\
\eta_4 &= Q_a^T C\gamma_\mu Q_b(\bar{q}_a\gamma^\mu\gamma_5 C\bar{q}_b^T - \bar{q}_b\gamma^\mu\gamma_5 C\bar{q}_a^T),\\
\eta_5 &= Q_a^T C\gamma_\mu\gamma_5 Q_b(\bar{q}_a\gamma^\mu C\bar{q}_b^T + \bar{q}_b\gamma^\mu C\bar{q}_a^T),
\end{aligned} \qquad (25)$$

  in which η_1, η_2, η_3 are isovector currents with $[\bar{\mathbf{6}}_\mathbf{f}]_{\bar{q}\bar{q}}$ and $I=1$, η_4, η_5 are isoscalar currents with $[\mathbf{3}_\mathbf{f}]_{\bar{q}\bar{q}}$ and $I=0$.

- For the currents with $J^P=0^+$,

$$\begin{aligned}
\eta_1&=Q_a^TCQ_b(\bar{q}_aC\bar{q}_b^T+\bar{q}_bC\bar{q}_b^T),\\
\eta_2&=Q_a^TC\gamma_5Q_b(\bar{q}_a\gamma_5C\bar{q}_b^T+\bar{q}_b\gamma_5C\bar{q}_b^T),\\
\eta_3&=Q_a^TC\gamma_\mu Q_b(\bar{q}_a\gamma^\mu C\bar{q}_b^T-\bar{q}_b\gamma^\mu C\bar{q}_b^T),\\
\eta_4&=Q_a^TC\gamma_\mu\gamma_5Q_b(\bar{q}_a\gamma^\mu\gamma_5C\bar{q}_b^T+\bar{q}_b\gamma^\mu\gamma_5C\bar{q}_b^T),\\
\eta_5&=Q_a^TC\sigma_{\mu\nu}Q_b(\bar{q}_a\sigma^{\mu\nu}C\bar{q}_b^T-\bar{q}_b\sigma^{\mu\nu}C\bar{q}_a^T),
\end{aligned}\tag{26}$$

  and all the scalar interpolating currents are isovector currents with $[\bar{\mathbf{6}}_\mathbf{f}]_{\bar{q}\bar{q}}$ and $I=1$.

- For the currents with $J^P=1^-$,

$$\begin{aligned}
\eta_1&=Q_a^TC\gamma_\mu\gamma_5Q_b(\bar{q}_a\gamma_5C\bar{q}_b^T+\bar{q}_b\gamma_5C\bar{q}_a^T),\\
\eta_2&=Q_a^TC\gamma_5Q_b(\bar{q}_a\gamma_\mu\gamma_5C\bar{q}_b^T+\bar{q}_b\gamma_\mu\gamma_5C\bar{q}_a^T),\\
\eta_3&=Q_a^TC\sigma_{\mu\nu}Q_b(\bar{q}_a\gamma^\nu C\bar{q}_b^T-\bar{q}_b\gamma^\nu C\bar{q}_a^T),\\
\eta_4&=Q_a^TC\gamma^\nu Q_b(\bar{q}_a\sigma_{\mu\nu}C\bar{q}_b^T-\bar{q}_b\sigma_{\mu\nu}C\bar{q}_a^T),\\
\eta_5&=Q_a^TC\gamma_\mu Q_b(\bar{q}_aC\bar{q}_b^T-\bar{q}_bC\bar{q}_a^T),\\
\eta_6&=Q_a^TCQ_b(\bar{q}_a\gamma_\mu C\bar{q}_b^T+\bar{q}_b\gamma_\mu C\bar{q}_a^T),\\
\eta_7&=Q_a^TC\sigma_{\mu\nu}\gamma_5Q_b(\bar{q}_a\gamma^\nu\gamma_5C\bar{q}_b^T-\bar{q}_b\gamma^\nu\gamma_5C\bar{q}_a^T),\\
\eta_8&=Q_a^TC\gamma^\nu\gamma_5Q_b(\bar{q}_a\sigma_{\mu\nu}\gamma_5C\bar{q}_b^T+\bar{q}_b\sigma_{\mu\nu}\gamma_5C\bar{q}_a^T),
\end{aligned}\tag{27}$$

  in which $\eta_1,\eta_2,\eta_3,\eta_4$ are isovector currents with $[\bar{\mathbf{6}}_\mathbf{f}]_{\bar{q}\bar{q}}$ and $I=1$, $\eta_5,\eta_6,\eta_7,\eta_8$ are isoscalar currents with $[\mathbf{3}_\mathbf{f}]_{\bar{q}\bar{q}}$ and $I=0$.

- For the currents with $J^P=1^+$,

$$\begin{aligned}
\eta_1&=Q_a^TC\gamma_\mu\gamma_5Q_b(\bar{q}_aC\bar{q}_b^T+\bar{q}_bC\bar{q}_a^T),\\
\eta_2&=Q_a^TCQ_b(\bar{q}_a\gamma_\mu\gamma_5C\bar{q}_b^T+\bar{q}_b\gamma_\mu\gamma_5C\bar{q}_a^T),\\
\eta_3&=Q_a^TC\sigma_{\mu\nu}\gamma_5Q_b(\bar{q}_a\gamma^\nu C\bar{q}_b^T-\bar{q}_b\gamma^\nu C\bar{q}_a^T),\\
\eta_4&=Q_a^TC\gamma^\nu Q_b(\bar{q}_a\sigma_{\mu\nu}\gamma_5C\bar{q}_b^T-\bar{q}_b\sigma_{\mu\nu}\gamma_5C\bar{q}_a^T),\\
\eta_5&=Q_a^TC\gamma_\mu Q_b(\bar{q}_a\gamma_5C\bar{q}_b^T-\bar{q}_b\gamma_5C\bar{q}_a^T),\\
\eta_6&=Q_a^TC\gamma_5Q_b(\bar{q}_a\gamma_\mu C\bar{q}_b^T+\bar{q}_b\gamma_\mu C\bar{q}_a^T),\\
\eta_7&=Q_a^TC\sigma_{\mu\nu}Q_b(\bar{q}_a\gamma^\nu\gamma_5C\bar{q}_b^T-\bar{q}_b\gamma^\nu\gamma_5C\bar{q}_a^T),\\
\eta_8&=Q_a^TC\gamma^\nu\gamma_5Q_b(\bar{q}_a\sigma_{\mu\nu}C\bar{q}_b^T+\bar{q}_b\sigma_{\mu\nu}C\bar{q}_a^T),
\end{aligned}\tag{28}$$

  in which $\eta_1,\eta_2,\eta_3,\eta_4$ are isovector currents with $[\bar{\mathbf{6}}_\mathbf{f}]_{\bar{q}\bar{q}}$ and $I=1$, $\eta_5,\eta_6,\eta_7,\eta_8$ are isoscalar currents with $[\mathbf{3}_\mathbf{f}]_{\bar{q}\bar{q}}$ and $I=0$.

In fact, the two pieces in the parenthesis of Eqs. (25)–(28) are equivalent to each other. We keep both of them here to illustrate the color symmetry explicitly. For these currents, we show their quark contents, spins, parities, isospins and the flavor symmetries of the light quark pair in Table III. The results of the spectral densities for these doubly charmed/bottomed tetraquark currents can be found in Ref. [55].

Quark Content	$[\bar{q}\bar{q}]_\mathbf{f}$	I	$J^P=0^-$	$J^P=0^+$	$J^P=1^-$	$J^P=1^+$
$QQ\bar{q}\bar{q}$	$\bar{\mathbf{6}}_\mathbf{f}$	1	η_1,η_2,η_3	$\eta_1,\eta_2,\eta_3,\eta_4,\eta_5$	$\eta_1,\eta_2,\eta_3,\eta_4$	$\eta_1,\eta_2,\eta_3,\eta_4$
$QQ\bar{s}\bar{s}$	$\bar{\mathbf{6}}_\mathbf{f}$	0	η_1,η_2,η_3	$\eta_1,\eta_2,\eta_3,\eta_4,\eta_5$	$\eta_1,\eta_2,\eta_3,\eta_4$	$\eta_1,\eta_2,\eta_3,\eta_4$
$QQ\bar{q}\bar{s}$	$\bar{\mathbf{6}}_\mathbf{f}$	1/2	$\eta_1,\eta_2,\eta_3,$	$\eta_1,\eta_2,\eta_3,\eta_4,\eta_5$	$\eta_1,\eta_2,\eta_3,\eta_4,$	$\eta_1,\eta_2,\eta_3,\eta_4,$
	$\mathbf{3}_\mathbf{f}$		η_4,η_5		$\eta_5,\eta_6,\eta_7,\eta_8$	$\eta_5,\eta_6,\eta_7,\eta_8$
$QQ\bar{u}\bar{d}$	$\mathbf{3}_\mathbf{f}$	0	η_4,η_5	$-$	$\eta_5,\eta_6,\eta_7,\eta_8$	$\eta_5,\eta_6,\eta_7,\eta_8$

TABLE III: Properties of the doubly charmed/bottomed tetraquark currents.

C. Open-flavor tetraquark $bc\bar{q}\bar{q}$ and $qc\bar{q}\bar{b}$ interpolating currents

In Ref. [56], the open-flavor tetraquark $bc\bar{q}\bar{q}$ and $qc\bar{q}\bar{b}$ interpolating currents with quantum numbers $J^P = 0^+, 1^+$ were constructed as follows.

- For the scalar $bc\bar{q}\bar{q}$ system with $J^P = 0^+$:

$$\begin{aligned}
J_1 &= b_a^T C\gamma_5 c_b (\bar{q}_a \gamma_5 C \bar{q}_b^T + \bar{q}_b \gamma_5 C \bar{q}_a^T), \\
J_2 &= b_a^T C\gamma_\mu c_b (\bar{q}_a \gamma^\mu C \bar{q}_b^T + \bar{q}_b \gamma^\mu C \bar{q}_a^T), \\
J_3 &= b_a^T C\gamma_5 c_b (\bar{q}_a \gamma_5 C \bar{q}_b^T - \bar{q}_b \gamma_5 C \bar{q}_a^T), \\
J_4 &= b_a^T C\gamma_\mu c_b (\bar{q}_a \gamma^\mu C \bar{q}_b^T - \bar{q}_b \gamma^\mu C \bar{q}_a^T),
\end{aligned} \tag{29}$$

  where J_1, J_2 have the symmetric color structure $[\mathbf{6_c}]_{bc} \otimes [\bar{\mathbf{6}}_\mathbf{c}]_{\bar{q}\bar{q}}$ and J_3, J_4 have the antisymmetric color structure $[\bar{\mathbf{3}}_\mathbf{c}]_{bc} \otimes [\mathbf{3_c}]_{\bar{q}\bar{q}}$.

- For the vector $bc\bar{q}\bar{q}$ system with $J^P = 1^+$:

$$\begin{aligned}
J_{1\mu} &= b_a^T C\gamma_5 c_b (\bar{q}_a \gamma_\mu C \bar{q}_b^T + \bar{q}_b \gamma_\mu C \bar{q}_a^T), \\
J_{2\mu} &= b_a^T C\gamma_\mu c_b (\bar{q}_a \gamma_5 C \bar{q}_b^T + \bar{q}_b \gamma_5 C \bar{q}_a^T), \\
J_{3\mu} &= b_a^T C\gamma_5 c_b (\bar{q}_a \gamma_\mu C \bar{q}_b^T - \bar{q}_b \gamma_\mu C \bar{q}_a^T), \\
J_{4\mu} &= b_a^T C\gamma_\mu c_b (\bar{q}_a \gamma_5 C \bar{q}_b^T - \bar{q}_b \gamma_5 C \bar{q}_a^T),
\end{aligned} \tag{30}$$

  where $J_{1\mu}, J_{2\mu}$ have the symmetric color structure $[\mathbf{6_c}]_{bc} \otimes [\bar{\mathbf{6}}_\mathbf{c}]_{\bar{q}\bar{q}}$ and $J_{3\mu}, J_{4\mu}$ have the antisymmetric color structure $[\bar{\mathbf{3}}_\mathbf{c}]_{bc} \otimes [\mathbf{3_c}]_{\bar{q}\bar{q}}$.

- For the scalar $cq\bar{b}\bar{q}$ system with $J^P = 0^+$:

$$\begin{aligned}
J_1 &= q_a^T C\gamma_5 c_b (\bar{q}_a \gamma_5 C \bar{b}_b^T + \bar{q}_b \gamma_5 C \bar{b}_a^T), \\
J_2 &= q_a^T C\gamma_\mu c_b (\bar{q}_a \gamma^\mu C \bar{b}_b^T + \bar{q}_b \gamma^\mu C \bar{b}_a^T), \\
J_3 &= q_a^T C\gamma_5 c_b (\bar{q}_a \gamma_5 C \bar{b}_b^T - \bar{q}_b \gamma_5 C \bar{b}_a^T), \\
J_4 &= q_a^T C\gamma_\mu c_b (\bar{q}_a \gamma^\mu C \bar{b}_b^T - \bar{q}_b \gamma^\mu C \bar{b}_a^T),
\end{aligned} \tag{31}$$

  where J_1, J_2 have the symmetric color structure $[\mathbf{6_c}]_{qc} \otimes [\bar{\mathbf{6}}_\mathbf{c}]_{\bar{q}\bar{b}}$ and J_3, J_4 have the antisymmetric color structure $[\bar{\mathbf{3}}_\mathbf{c}]_{qc} \otimes [\mathbf{3_c}]_{\bar{q}\bar{b}}$.

- For the vector $cq\bar{b}\bar{q}$ system with $J^P = 1^+$:

$$\begin{aligned}
J_{1\mu} &= q_a^T C\gamma_5 c_b (\bar{q}_a \gamma_\mu C \bar{b}_b^T + \bar{q}_b \gamma_\mu C \bar{b}_a^T), \\
J_{2\mu} &= q_a^T C\gamma_\mu c_b (\bar{q}_a \gamma_5 C \bar{b}_b^T + \bar{q}_b \gamma_5 C \bar{b}_a^T), \\
J_{3\mu} &= q_a^T C\gamma_5 c_b (\bar{q}_a \gamma_\mu C \bar{b}_b^T - \bar{q}_b \gamma_\mu C \bar{b}_a^T), \\
J_{4\mu} &= q_a^T C\gamma_\mu c_b (\bar{q}_a \gamma_5 C \bar{b}_b^T - \bar{q}_b \gamma_5 C \bar{b}_a^T),
\end{aligned} \tag{32}$$

  where $J_{1\mu}, J_{2\mu}$ have the symmetric color structure $[\mathbf{6_c}]_{qc} \otimes [\bar{\mathbf{6}}_\mathbf{c}]_{\bar{q}\bar{b}}$ and $J_{3\mu}, J_{4\mu}$ have the antisymmetric color structure $[\bar{\mathbf{3}}_\mathbf{c}]_{qc} \otimes [\mathbf{3_c}]_{\bar{q}\bar{b}}$.

The $cs\bar{b}\bar{s}$ tetraquark currents with $J^P = 0^+, 1^+$ are the same as the $cq\bar{b}\bar{q}$ currents in Eqs. (31) and (32) respectively, by replacing the light quark q by the strange quark s. For the $bc\bar{s}\bar{s}$ systems, the flavor structure of $\bar{s}\bar{s}$ pair is symmetric. Thus the color structures for the diquark fields $s_a^T C\gamma_5 s_b$ and $s_a^T C\gamma_\mu s_b$ are symmetric $\mathbf{6_c}$ and antisymmetric $\bar{\mathbf{3}}_\mathbf{c}$, respectively. As a result, only J_1, J_4 in Eq. (29) and $J_{2\mu}$, $J_{3\mu}$ in Eq. (30) survive in the $bc\bar{s}\bar{s}$ system. The spectral densities for these open-flavor tetraquark currents were calculated and listed in Ref. [56].

D. Quarkonium hybrid $\bar{Q}GQ$ interpolating currents

The quarkonium hybrids were originally studied in Refs. [30–32] in the QCD sum rules method. However, it was shown that only the hybrid channels with $J^{PC}=0^{--},0^{++},1^{+-},1^{++},2^{++}$ gave stable mass sum rules while the sum rules in the $J^{PC}=0^{-+},0^{+-},1^{-+},1^{--},2^{-+}$ channels were unstable. Recently, new efforts on the quarkonium hybrid mesons have found that the dimension six tri-gluon condensate can stabilize the hybrid sum rules [34–38].

To study the hybrid correlation functions, we consider the following interpolating currents with various quantum numbers:

$$\begin{aligned} J^{(1)}_{\mu} &= g_s\bar{Q}_1\frac{\lambda^a}{2}\gamma^{\nu}G^a_{\mu\nu}Q_2, \qquad J^{P(C)}=1^{-(+)},0^{+(+)}, \\ J^{(2)}_{\mu} &= g_s\bar{Q}_1\frac{\lambda^a}{2}\gamma^{\nu}\gamma_5 G^a_{\mu\nu}Q_2, \qquad J^{P(C)}=1^{+(-)},0^{-(-)}, \\ J^{(3)}_{\mu\nu} &= g_s\bar{Q}_1\frac{\lambda^a}{2}\sigma^{\alpha}_{\mu}\gamma_5 G^a_{\alpha\nu}Q_2, \qquad J^{P(C)}=2^{-(+)},1^{+(+)},1^{-(+)},0^{-(+)}, \end{aligned} \tag{33}$$

in which Q_1 and Q_2 are the heavy quark fields with masses m_1 and m_2, g_s is the strong coupling constant, λ^a are the Gell-Mann SU(3) matrices and $G^a_{\mu\nu}$ is the gluon field strength. It should be understood that the operators in Eq. (33) contain the hidden charm/bottom hybrid currents with $Q_1=Q_2$ carrying C-parities in the parentheses and the open-flavor $\bar{b}Gc$ hybrid currents with $Q_1\neq Q_2$ carrying no definite C-parities. By replacing $G^a_{\mu\nu}$ with $\tilde{G}^a_{\mu\nu}=\frac{1}{2}\epsilon_{\mu\nu\alpha\beta}G^{\alpha\beta,a}$, one can also obtain the operators $\tilde{J}^{(1)}_{\mu}, \tilde{J}^{(2)}_{\mu}, \tilde{J}^{(3)}_{\mu\nu}$ coupling to the hybrid states with the opposite parities to $J^{(1)}_{\mu}, J^{(2)}_{\mu}, J^{(3)}_{\mu\nu}$ respectively. The correlation functions and spectral densities are calculated up to dimension six tri-gluon condensate at leading order in α_s. We will discuss the importance of the tri-gluon condensate in the next section. The results of the spectral densities are listed in Refs. [37, 38].

IV. MASS SPECTRUM OF THE QUARKONIUMLIKE TETRAQUARK $qQ\bar{q}\bar{Q}$ STATES

The QCD sum rule study of the $qQ\bar{q}\bar{Q}$ systems was performed in Refs. [51, 52], using the interpolating currents in Eqs. (22)–(24). As introduced in Sec. I, the charmoniumlike tetraquark states are good candidates for some newly observed XYZ resonances. For example, the $Y(4660)$ meson was first observed by Belle in the $e^+e^-\to\gamma_{ISR}Y(4660)\to\gamma_{ISR}\psi(2S)\pi^+\pi^-$ process [91]. Since it was observed in the initial state radiation (ISR) process, its quantum number is $J^{PC}=1^{--}$. The tetraquark interpolating current for such quantum numbers is given in Eq. (23).

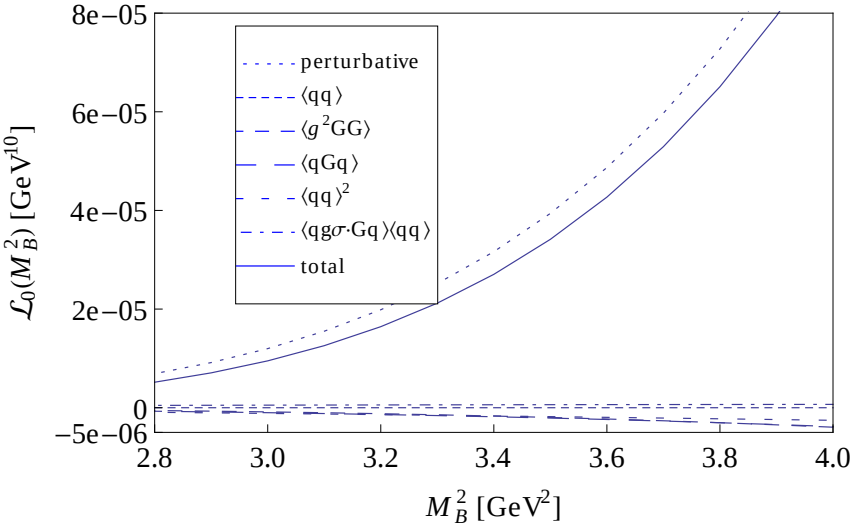

FIG. 1: OPE convergence for $J_{1\mu}$ with $J^{PC}=1^{--}$ in the $qc\bar{q}\bar{c}$ systems.

For the $qc\bar{q}\bar{c}$ currents $J_{1\mu}$ with $J^{PC}=1^{--}$ in Eq. (23), we show the convergence of the OPE series in Fig. 1. We see that the four-quark condensate $\langle\bar{q}q\rangle^2$ is the most important nonperturbative contribution to the correlation function. In fact, the quark condensate $\langle\bar{q}q\rangle$ is proportional to the light quark mass and vanishes in the limit $m_q=0$. The

OPE convergence is very good in the region $M_B^2 \geq 2.9$ GeV^2. To study the pole contribution defined in Eq. (14), one should determine the continuum threshold s_0. In the left portion of Fig. 2, the hadron mass m_X is extracted as a function of s_0. One can find a plateau in the region 10 GeV$^2 \leq s_0 \leq 14$ GeV^2. However, this is a non-physical artifact because the spectral density of the sum rules defined in Eq. (12) is negative in this region. The variation of m_X with the Borel mass M_B^2 is weak around $s_0 = 25$ GeV^2. Using this value of the continuum threshold, we study the pole contribution and require that PC be larger than 40%, which results in an upper bound of the Borel mass $M_{\rm max}^2 = 3.6$ GeV^2.

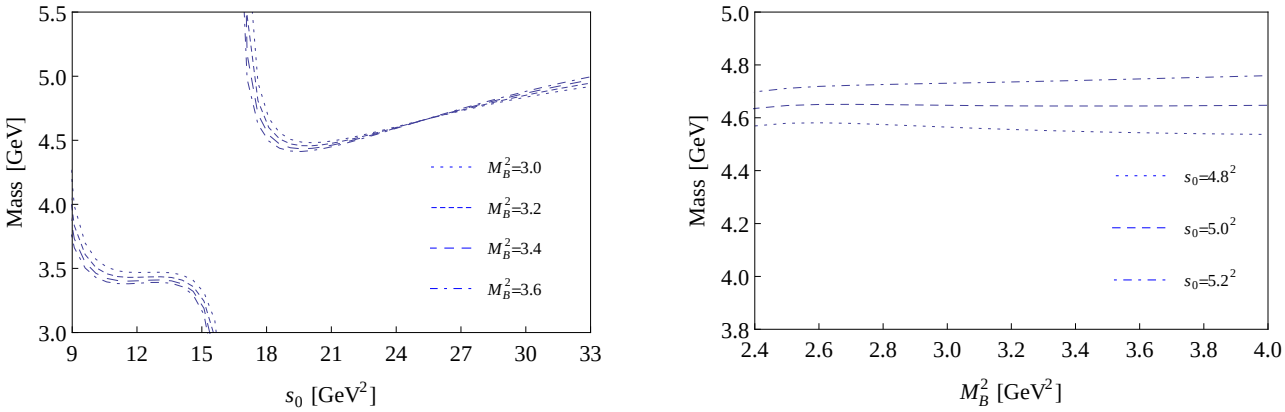

FIG. 2: Variations of m_X with s_0 and M_B^2 for $J_{1\mu}$ with $J^{PC} = 1^{--}$ in the $qc\bar{q}\bar{c}$ systems.

In the right portion of Fig. 2, we show the variation of m_X with M_B^2 for $J_{1\mu}$ with $J^{PC} = 1^{--}$ in the $qc\bar{q}\bar{c}$ systems. The curves are very stable in the Borel window 2.9 GeV$^2 \leq M_B^2 \leq 3.6$ GeV^2. The hadron mass is then extracted as

$$m_X = (4.64 \pm 0.09)\text{GeV}, \tag{34}$$

which is consistent with the mass of the $Y(4660)$ meson. This result implies a possible tetraquark interpretation of $Y(4660)$. However, the tetraquark state can decay easily into two meson final states via the rearrangement mechanism so it is very difficult to explain the small decay width of the $Y(4660)$ meson. The $Y(4660)$ was also considered as a $f_0(980)\psi'$ bound state [92], a baryonium state [93], a 5 $^3S_1 c\bar{c}$ state [94] and a $sc\bar{s}\bar{c}$ tetraquark state [95, 96].

We can study the corresponding $sc\bar{s}\bar{c}$ state by replacing the light quarks in the interpolating current by a strange quark. The quark condensate $\langle\bar{s}s\rangle$ is now proportional to the strange quark mass m_s. Its contribution is larger than the four-quark condensate $\langle\bar{s}s\rangle^2$ and becomes the dominant power correction for the 1^{--} $sc\bar{s}\bar{c}$ system. The extracted mass of this state is [51]:

$$m_{X^s} = (4.92 \pm 0.10)\text{GeV}, \tag{35}$$

which is 0.28 GeV higher than the 1^{--} $qc\bar{q}\bar{c}$ state.

Properties of the bottomoniumlike analogues are very similar due to the heavy quark symmetry. Replacing the charm quark by the bottom quark in the current and repeating the same analysis procedures, we can also extract the masses of the $qb\bar{q}\bar{b}$ and $sb\bar{s}\bar{b}$ tetraquark states with $J^{PC} = 1^{--}$. After performing the QCD sum rule analysis for all the interpolating currents in Eqs. (22)–(24), we obtained the numerical results for $J^{PC} = 0^{--}, 0^{-+}, 1^{-+}, 1^{--}, 1^{++}$ and 1^{+-} tetraquark systems in Tables IV, V, VI, VII, VIII and IX, respectively [51, 52]. Only the errors from the uncertainty of the threshold values and variation of the Borel parameter are taken into account. Other possible error sources include the truncation of the OPE series and the uncertainty of the quark masses, condensate values and so on. We only collect the numerical results from the interpolating currents which lead to stable mass sum rules and reliable mass predictions in these tables. The tetraquark states with $J^{PC} = 0^{--}$ and 1^{-+} are exotic states. They do not mix with the conventional charmonium and bottomonium states because these quantum numbers are not accessible to simple $q\bar{q}$ states.

	Currents	s_0(GeV^2)	$[M_{\rm min}^2, M_{\rm max}^2]$(GeV^2)	m_X(GeV)	PC(%)
$J^{PC} = 0^{--}$	J_2	25	$2.4 - 3.7$	4.55 ± 0.11	46.3
	J_4	25	$2.4 - 3.7$	4.55 ± 0.11	45.9

TABLE IV: Numerical results for the $qc\bar{q}\bar{c}$ tetraquark states with $J^{PC} = 0^{--}$.

	Currents	$s_0(\text{GeV}^2)$	$[M^2_{\text{min}}, M^2_{\text{max}}](\text{GeV}^2)$	$m_X(\text{GeV})$	PC(%)
$J^{PC}=0^{-+}$	J_2	27	$2.4-4.1$	4.72 ± 0.10	53.8
	J_5	25	$2.4-3.7$	4.55 ± 0.11	45.9
	J_6	27	$2.4-4.2$	4.67 ± 0.10	56.8

TABLE V: Numerical results for the $qc\bar{q}\bar{c}$ tetraquark states with $J^{PC}=0^{-+}$.

	Currents	$s_0(\text{GeV}^2)$	$[M^2_{\text{min}}, M^2_{\text{max}}](\text{GeV}^2)$	$m_X(\text{GeV})$	PC(%)
$qc\bar{q}\bar{c}$ system	$J_{6\mu}$	5.1^2	$2.9-3.9$	4.67 ± 0.10	50.2
	$J_{7\mu}$	5.2^2	$2.9-4.2$	4.77 ± 0.10	47.4
	$J_{8\mu}$	4.9^2	$2.9-3.4$	4.53 ± 0.10	46.3
$sc\bar{s}\bar{c}$ system	$J_{1\mu}$	5.0^2	$2.9-3.4$	4.67 ± 0.10	44.3
	$J_{2\mu}$	5.0^2	$2.9-3.4$	4.65 ± 0.09	45.6
	$J_{3\mu}$	4.9^2	$2.9-3.3$	4.54 ± 0.10	44.4
	$J_{4\mu}$	5.1^2	$2.9-3.7$	4.72 ± 0.09	44.8
	$J_{5\mu}$	5.0^2	$2.9-3.6$	4.62 ± 0.10	42.8
	$J_{6\mu}$	5.3^2	$2.9-4.3$	4.84 ± 0.10	47.3
	$J_{7\mu}$	5.3^2	$2.9-4.3$	4.87 ± 0.10	46.2
	$J_{8\mu}$	5.2^2	$2.9-4.1$	4.77 ± 0.10	44.1
$qb\bar{q}\bar{b}$ system	$J_{6\mu}$	11.0^2	$7.2-8.6$	10.53 ± 0.11	44.2
	$J_{7\mu}$	11.0^2	$7.2-8.6$	10.53 ± 0.10	44.1
	$J_{8\mu}$	11.0^2	$7.2-8.6$	10.49 ± 0.11	44.7
$sb\bar{s}\bar{b}$ system	$J_{4\mu}$	11.0^2	$7.2-8.1$	10.62 ± 0.10	41.2
	$J_{5\mu}$	11.0^2	$7.2-8.4$	10.56 ± 0.10	43.8
	$J_{6\mu}$	11.0^2	$7.2-8.3$	10.63 ± 0.10	42.4
	$J_{7\mu}$	11.0^2	$7.2-8.3$	10.62 ± 0.09	42.5
	$J_{8\mu}$	11.0^2	$7.2-8.3$	10.59 ± 0.10	43.1

TABLE VI: Numerical results for the $qc\bar{q}\bar{c}$, $sc\bar{s}\bar{c}$, $qb\bar{q}\bar{b}$ and $sb\bar{s}\bar{b}$ tetraquark states with $J^{PC}=1^{-+}$.

	Currents	$s_0(\text{GeV}^2)$	$[M^2_{\text{min}},M^2_{\text{max}}](\text{GeV}^2)$	$m_X(\text{GeV})$	PC(%)
	$J_{1\mu}$	5.0^2	$2.9-3.6$	4.64 ± 0.09	44.1
$qc\bar{q}\bar{c}$ system	$J_{4\mu}$	5.0^2	$2.9-3.6$	4.61 ± 0.10	46.4
	$J_{7\mu}$	5.2^2	$2.9-4.1$	4.74 ± 0.10	47.3
	$J_{1\mu}$	5.4^2	$2.8-4.5$	4.92 ± 0.10	50.3
	$J_{2\mu}$	5.0^2	$2.8-3.5$	4.64 ± 0.09	48.6
$sc\bar{s}\bar{c}$ system	$J_{3\mu}$	4.9^2	$2.8-3.4$	4.52 ± 0.10	45.6
	$J_{4\mu}$	5.4^2	$2.8-4.5$	4.88 ± 0.10	51.7
	$J_{7\mu}$	5.3^2	$2.8-4.3$	4.86 ± 0.10	46.0
	$J_{8\mu}$	4.8^2	$2.8-3.1$	4.48 ± 0.10	43.2
$qb\bar{q}\bar{b}$ system	$J_{7\mu}$	11.0^2	$7.2-8.5$	10.51 ± 0.10	45.8
	$J_{1\mu}$	11.0^2	$7.2-8.3$	10.60 ± 0.10	47.0
	$J_{2\mu}$	11.0^2	$7.2-8.4$	10.55 ± 0.11	43.6
$sb\bar{s}\bar{b}$ system	$J_{3\mu}$	11.0^2	$7.2-8.4$	10.55 ± 0.10	43.7
	$J_{4\mu}$	11.0^2	$7.2-8.4$	10.53 ± 0.11	44.3
	$J_{7\mu}$	11.0^2	$7.2-8.2$	10.62 ± 0.10	42.0
	$J_{8\mu}$	11.0^2	$7.2-8.4$	10.53 ± 0.10	44.1

TABLE VII: Numerical results for the $qc\bar{q}\bar{c}$, $sc\bar{s}\bar{c}$, $qb\bar{q}\bar{b}$ and $sb\bar{s}\bar{b}$ tetraquark states with $J^{PC}=1^{--}$.

	Currents	$s_0(\text{GeV}^2)$	$[M^2_{\text{min}},M^2_{\text{max}}](\text{GeV}^2)$	$m_X(\text{GeV})$	PC(%)
$qc\bar{q}\bar{c}$ system	$J_{3\mu}$	4.6^2	$3.0-3.4$	4.19 ± 0.10	47.3
	$J_{4\mu}$	4.5^2	$3.0-3.3$	4.03 ± 0.11	46.8
$sc\bar{s}\bar{c}$ system	$J_{3\mu}$	4.6^2	$3.0-3.4$	4.22 ± 0.10	45.7
	$J_{4\mu}$	4.5^2	$3.0-3.3$	4.07 ± 0.10	44.4
	$J_{3\mu}$	10.9^2	$8.5-9.5$	10.32 ± 0.09	47.0
$qb\bar{q}\bar{b}$ system	$J_{4\mu}$	10.8^2	$8.5-9.2$	10.22 ± 0.11	44.6
	$J_{7\mu}$	10.7^2	$7.8-8.4$	10.14 ± 0.10	44.8
	$J_{8\mu}$	10.7^2	$7.8-8.4$	10.14 ± 0.09	44.8
	$J_{3\mu}$	10.9^2	$8.5-9.5$	10.34 ± 0.09	46.1
$sb\bar{s}\bar{b}$ system	$J_{4\mu}$	10.8^2	$8.5-9.1$	10.25 ± 0.10	43.3
	$J_{7\mu}$	10.8^2	$7.5-8.6$	10.24 ± 0.11	47.1
	$J_{8\mu}$	10.8^2	$7.5-8.6$	10.24 ± 0.10	47.1

TABLE VIII: Numerical results for the $qc\bar{q}\bar{c}$, $sc\bar{s}\bar{c}$, $qb\bar{q}\bar{b}$ and $sb\bar{s}\bar{b}$ tetraquark states with $J^{PC}=1^{++}$.

	Currents	$s_0(\mathrm{GeV}^2)$	$[M^2_{\rm min},M^2_{\rm max}](\mathrm{GeV}^2)$	$m_X(\mathrm{GeV})$	PC(%)
	$J_{3\mu}$	4.6^2	$3.0-3.4$	4.16 ± 0.10	46.2
$qc\bar{q}\bar{c}$ system	$J_{4\mu}$	4.5^2	$3.0-3.3$	4.02 ± 0.09	44.6
	$J_{5\mu}$	4.5^2	$3.0-3.4$	4.00 ± 0.11	46.0
	$J_{6\mu}$	4.6^2	$3.0-3.4$	4.14 ± 0.09	47.0
	$J_{3\mu}$	4.7^2	$3.0-3.6$	4.24 ± 0.10	49.6
$sc\bar{s}\bar{c}$ system	$J_{4\mu}$	4.6^2	$3.0-3.5$	4.12 ± 0.11	47.3
	$J_{5\mu}$	4.5^2	$3.0-3.3$	4.03 ± 0.11	44.2
	$J_{6\mu}$	4.6^2	$3.0-3.4$	4.16 ± 0.11	46.0
	$J_{3\mu}$	10.6^2	$7.5-8.5$	10.08 ± 0.10	45.9
$qb\bar{q}\bar{b}$ system	$J_{4\mu}$	10.6^2	$7.5-8.5$	10.07 ± 0.10	46.2
	$J_{5\mu}$	10.6^2	$7.5-8.4$	10.05 ± 0.10	45.3
	$J_{6\mu}$	10.7^2	$7.5-8.7$	10.15 ± 0.10	47.6
	$J_{3\mu}$	10.6^2	$7.5-8.3$	10.11 ± 0.10	43.8
$sb\bar{s}\bar{b}$ system	$J_{4\mu}$	10.6^2	$7.5-8.4$	10.10 ± 0.10	44.1
	$J_{5\mu}$	10.6^2	$7.5-8.3$	10.08 ± 0.10	43.7
	$J_{6\mu}$	10.7^2	$7.5-8.5$	10.18 ± 0.10	46.5

TABLE IX: Numerical results for the $qc\bar{q}\bar{c}$, $sc\bar{s}\bar{c}$, $qb\bar{q}\bar{b}$ and $sb\bar{s}\bar{b}$ tetraquark states with $J^{PC}=1^{+-}$.

The $X(3872)$ is the first observed XYZ state [97] and its quantum number was assigned as $J^{PC}=1^{++}$[98]. The mass and decay mode of $X(3872)$ are very different from that of the 2^3P_1 $c\bar{c}$ state. To date, the possible interpretations of $X(3872)$ include the molecular state [99–105], tetraquark state [48–50], cusp [106], hybrid charmonium [107] and mixed scenarios [108, 109]. In Table VIII, the masses of the 1^{++} $qc\bar{q}\bar{c}$ states are $m_X=4.0-4.2$ GeV, in rough agreement with the mass of the $X(3872)$, considering the uncertainties.

Recently, BESIII collaboration discovered a charged charmoniumlike resonance $Z_c(4025)$ in the process $e^+e^-\to(D^*\bar{D}^*)^{\pm}\pi^{\mp}$ [113]. The quantum numbers of $Z_c(4025)$ was $I^G(J^P)=1^+(1^+)$ because it was also observed in $h_c\pi$ channel. Its neutral partner carries the negative C-parity. Therefore its quantum number is $J^{PC}=1^{+-}$. The extracted masses of the $qc\bar{q}\bar{c}$ states with $J^{PC}=1^{+-}$ in Table IX and 1^{++} in Table VIII are about $m_X=4.0-4.2$ GeV, which supports $Z_c(4025)$ as a $I^G(J^P)=1^+(1^+)$ tetraquark candidate. The $Z_c(4025)$ were also studied as a $D^*\bar{D}^*$ molecular state [114–117], a $[cu][\bar{c}\bar{d}]$ tetraquark with the quantum numbers $J^P=2^+$ [118].

V. MASS SPECTRUM OF THE DOUBLY CHARMED/BOTTOMED TETRAQUARK $QQ\bar{q}\bar{q}$ STATES

The interpolating currents of the doubly charmed/bottomed $QQ\bar{q}\bar{q}$ systems are listed in Eqs. (25)–(28). For all the isovector $QQ\bar{q}\bar{q}$ and isoscalar $QQ\bar{u}\bar{d}$ systems, the dominant power corrections are the four-quark condensate $\langle\bar{q}q\rangle^2$. Both the quark condensate and the quark-gluon mixed condensate are proportional to the light quark mass and hence are chirally suppressed.

In Fig. 3, we show the variations of m_X with M_B and s_0 for the current η_3 with $(I,J^P)=(1,0^-)$ in $cc\bar{q}\bar{q}$ system. The mass curves for the different values of the Borel mass intersect at $s_0=23$ GeV^2, at which the variation of m_X with M_B^2 is very weak. After studying the OPE convergence and the pole contribution, we obtain the Borel window 2.6 GeV$^2\leq M_B^2\leq$ 3.6 GeV^2 in which the mass curves are very stable, as shown in the left part of Fig. 3. The mass was extracted around $m_X=(4.47\pm0.12)$ GeV [55]. The situation is very different from the $(I,J^P)=(1,0^-)$ in the $cc\bar{s}\bar{s}$ systems. The quark condensate $\langle\bar{s}s\rangle$ becomes the dominant power correction in these systems by keeping the m_s dependent terms in the spectral densities. To compare with the $cc\bar{q}\bar{q}$ system, we show the variations of m_{X^s} with M_B^2 and s_0 for the current η_3^s in Fig. 4. The quark condensate and the quark-gluon mixed condensate enhanced the pole contribution, which resulted in a broader Borel window 2.7 GeV$^2\leq M_B^2\leq$ 4.3 GeV^2. The extracted mass was $m_{X^s}=(4.79\pm0.17)$ GeV, which is about $2m_s$ higher than the $cc\bar{q}\bar{q}$ state [55].

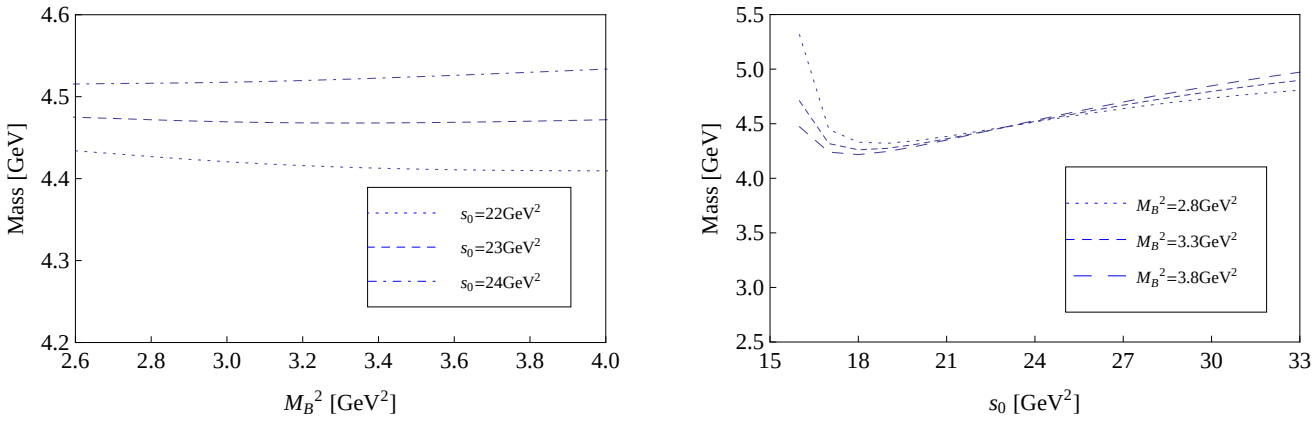

FIG. 3: Variations of m_X with M_B and s_0 for the current η_3 with $(I, J^P) = (1, 0^-)$ in $cc\bar{q}\bar{q}$ system.

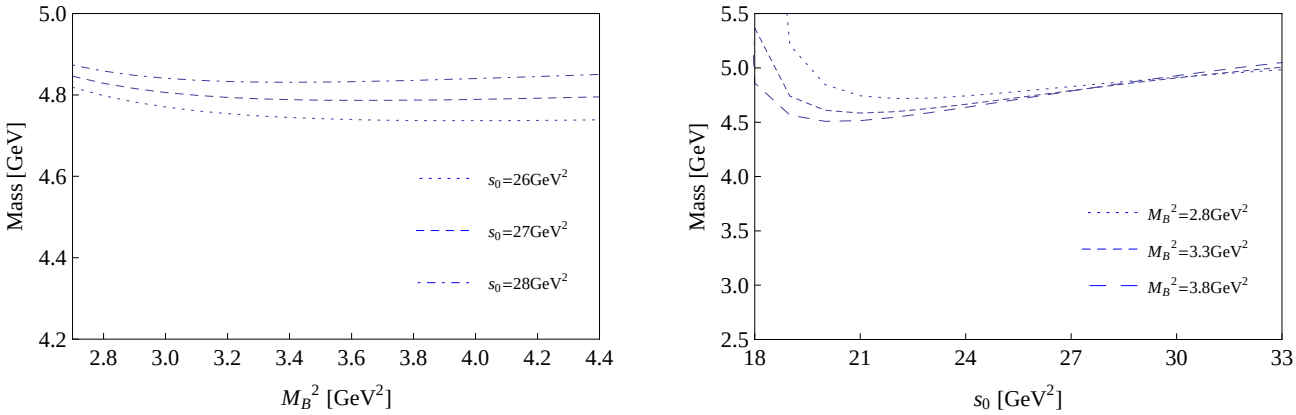

FIG. 4: Variations of m_{X^s} with M_B and s_0 for the current η_3^s with $(I, J^P) = (0, 0^-)$ in $cc\bar{s}\bar{s}$ system.

	Current	s_0 (GeV^2)	$[M^2_{Bmin}, M^2_{Bmax}]$ (GeV^2)	M_B^2 (GeV^2)	m_X (GeV)	PC (%)	f_X (GeV^5)	open charm/bottom threshold (GeV)
$cc\bar{q}\bar{q}$	η_1	24	$3.0-3.9$	3.4	4.43 ± 0.12	41.2	0.0674	
	η_3	23	$2.6-3.6$	3.1	4.47 ± 0.12	42.6	0.312	3.872
$cc\bar{u}\bar{d}$	η_4	22	$2.7-3.4$	3.0	4.43 ± 0.13	38.4	0.0870	
	η_5	23	$2.5-3.7$	3.2	4.41 ± 0.14	41.5	0.106	
$cc\bar{q}\bar{s}$	η_1	24	$2.9-3.8$	3.4	4.45 ± 0.16	40.1	0.0489	
	η_2	24	$2.7-3.7$	3.4	4.68 ± 0.12	43.1	0.106	
	η_3	26	$3.0-4.4$	3.8	4.71 ± 0.14	40.6	0.245	3.975
	η_4	25	$2.6-4.1$	3.4	4.64 ± 0.13	44.9	0.136	
	η_5	24	$2.6-4.1$	3.4	4.50 ± 0.16	45.9	0.124	
$cc\bar{s}\bar{s}$	η_1	25	$2.8-4.0$	3.4	4.46 ± 0.13	44.3	0.0731	4.081
	η_3	27	$2.7-4.3$	3.4	4.79 ± 0.17	47.7	0.558	
$bb\bar{q}\bar{q}$	η_1	125	$7.0-9.6$	8.0	10.6 ± 0.3	48.6	0.207	
	η_3	120	$6.8-9.4$	8.0	10.5 ± 0.3	43.7	1.60	10.60
$bb\bar{u}\bar{d}$	η_5	115	$7.0-8.1$	7.5	10.3 ± 0.2	36.5	0.367	
$bb\bar{q}\bar{s}$	η_1	124	$7.2-9.6$	8.5	10.6 ± 0.2	40.8	0.188	
	η_3	120	$7.2-9.1$	8.0	10.6 ± 0.2	40.2	0.853	10.69
	η_5	115	$7.0-7.9$	7.5	10.4 ± 0.2	33.8	0.378	
$bb\bar{s}\bar{s}$	η_1	125	$6.7-9.6$	8.0	10.6 ± 0.3	47.9	0.286	10.78
	η_3	120	$6.6-8.9$	8.0	10.6 ± 0.3	38.0	1.74	

TABLE X: The numerical results for the doubly-charmed/bottomed $QQ\bar{q}\bar{q}$, $QQ\bar{u}\bar{d}$, $QQ\bar{q}\bar{s}$ and $QQ\bar{s}\bar{s}$ systems with $J^P=0^-$.

	Current	s_0 (GeV^2)	$[M^2_{Bmin}, M^2_{Bmax}]$ (GeV^2)	M_B^2 (GeV^2)	m_X (GeV)	PC (%)	f_X (GeV^5)	open charm/bottom threshold (GeV)
$cc\bar{q}\bar{s}$	η_2	22	$2.8-3.6$	3.2	4.16 ± 0.14	39.0	0.0548	3.833
	η_3	20	$2.6-3.4$	3.0	4.02 ± 0.18	39.3	0.0561	
$cc\bar{s}\bar{s}$	η_1	28	$3.2-4.1$	3.4	5.05 ± 0.15	43.3	0.136	3.937
	η_2	22	$2.6-3.8$	3.2	4.27 ± 0.11	43.2	0.0933	
$bb\bar{q}\bar{q}$	η_2	120	$7.0-9.8$	8.2	10.3 ± 0.3	48.2	0.590	
	η_3	115	$6.9-9.0$	8.0	10.2 ± 0.3	40.3	0.539	10.56
	η_5	115	$6.7-8.8$	8.0	10.2 ± 0.3	39.4	1.10	
$bb\bar{q}\bar{s}$	η_3	115	$6.5-8.8$	8.0	10.2 ± 0.3	40.3	0.398	
	η_4	115	$5.8-8.6$	7.2	10.2 ± 0.3	45.6	0.337	10.65
	η_5	120	$6.2-9.8$	8.0	10.3 ± 0.3	49.3	0.806	
$bb\bar{s}\bar{s}$	η_1	130	$7.5-9.8$	8.5	11.0 ± 0.2	41.4	0.391	
	η_2	120	$6.4-9.8$	8.0	10.4 ± 0.3	49.7	0.632	
	η_3	115	$6.3-9.0$	8.0	10.2 ± 0.3	40.5	0.560	10.73
	η_4	120	$6.2-8.4$	8.0	10.4 ± 0.3	41.9	0.486	
	η_5	115	$6.2-8.8$	8.0	10.2 ± 0.3	38.9	1.14	

TABLE XI: Numerical results for the doubly-charmed/bottomed $QQ\bar{q}\bar{q}$, $QQ\bar{u}\bar{d}$, $QQ\bar{q}\bar{s}$ and $QQ\bar{s}\bar{s}$ systems with $J^P=0^+$.

	Current	s_0 (GeV^2)	$[M^2_{Bmin}, M^2_{Bmax}]$ (GeV^2)	M_B^2 (GeV^2)	m_X (GeV)	PC (%)	f_X (GeV^5)	open charm/bottom threshold (GeV)
$cc\bar{q}\bar{q}$	η_1	23	$3.0-3.6$	3.3	4.35 ± 0.14	38.6	0.0490	
$cc\bar{u}\bar{d}$	η_6	23	$3.1-3.7$	3.4	4.34 ± 0.16	37.9	0.0395	3.730
	η_7	22	$2.6-3.4$	3.0	4.41 ± 0.12	39.4	0.0690	
	η_8	23	$2.6-3.5$	3.0	4.42 ± 0.14	41.1	0.0940	
$cc\bar{q}\bar{s}$	η_1	23	$2.7-3.6$	3.2	4.37 ± 0.17	39.1	0.0357	
	η_2	24	$2.9-3.8$	3.2	4.59 ± 0.13	43.0	0.0838	
	η_6	23	$2.9-3.7$	3.4	4.35 ± 0.16	37.7	0.0353	3.833
	η_7	24	$2.4-3.9$	3.4	4.58 ± 0.14	39.8	0.105	
	η_8	24	$2.4-3.9$	3.4	4.52 ± 0.13	41.1	0.114	
	η_1	24	$2.8-3.7$	3.3	4.47 ± 0.13	40.7	0.0603	
$cc\bar{s}\bar{s}$	η_3	23	$2.5-3.5$	3.0	4.47 ± 0.14	40.9	0.101	3.937
	η_4	26	$2.8-4.2$	3.3	4.74 ± 0.17	49.1	0.196	
$bb\bar{q}\bar{q}$	η_1	125	$7.0-9.6$	8.0	10.6 ± 0.3	47.8	0.229	
$bb\bar{u}\bar{d}$	η_6	120	$7.2-8.9$	8.0	10.4 ± 0.2	40.5	0.142	10.56
	η_8	120	$8.2-9.4$	8.8	10.5 ± 0.2	35.9	0.492	
	η_1	120	$7.2-8.8$	8.0	10.5 ± 0.2	37.9	0.124	
$bb\bar{q}\bar{s}$	η_6	120	$7.2-8.9$	8.0	10.4 ± 0.2	40.6	0.145	10.65
	η_8	120	$7.6-9.3$	8.4	10.5 ± 0.2	37.8	0.491	
	η_1	125	$6.6-9.6$	8.0	10.6 ± 0.3	47.1	0.240	
$bb\bar{s}\bar{s}$	η_3	120	$6.7-9.0$	8.0	10.5 ± 0.3	40.1	0.490	10.73
	η_4	120	$6.8-8.9$	8.0	10.6 ± 0.3	38.8	0.655	

TABLE XII: Numerical results for the doubly-charmed/bottomed $QQ\bar{q}\bar{q}$, $QQ\bar{u}\bar{d}$, $QQ\bar{q}\bar{s}$ and $QQ\bar{s}\bar{s}$ systems with $J^P = 1^-$.

	Current	s_0 (GeV^2)	$[M^2_{Bmin}, M^2_{Bmax}]$ (GeV^2)	M_B^2 (GeV^2)	m_X (GeV)	PC (%)	f_X (GeV^5)	open charm/bottom threshold (GeV)
	η_1	28	$3.0-4.2$	3.6	4.96 ± 0.11	42.1	0.0801	
	η_2	27	$3.1-4.0$	3.6	4.87 ± 0.11	38.5	0.0726	
$cc\bar{q}\bar{s}$	η_3	21	$2.4-3.4$	2.8	4.12 ± 0.17	47.5	0.0571	
	η_4	21	$2.5-3.4$	2.8	4.13 ± 0.16	47.9	0.0574	3.975
	η_5	21	$2.8-3.7$	3.2	4.12 ± 0.16	41.7	0.0378	
	η_6	21	$3.0-3.7$	3.2	4.17 ± 0.12	41.5	0.0718	
	η_7	21	$2.2-3.3$	2.8	4.15 ± 0.17	42.9	0.0465	
$cc\bar{s}\bar{s}$	η_1	29	$3.2-4.5$	3.8	5.03 ± 0.13	42.5	0.138	
	η_2	30	$3.2-4.6$	3.8	5.12 ± 0.14	45.9	0.150	4.081
	η_3	21	$2.2-3.4$	2.8	4.17 ± 0.16	45.4	0.0838	
	η_4	21	$2.2-3.4$	2.8	4.19 ± 0.16	45.7	0.0849	
$bb\bar{q}\bar{q}$	η_3	115	$6.5-8.8$	7.8	10.2 ± 0.3	41.4	0.459	
	η_4	115	$6.8-8.8$	7.8	10.2 ± 0.3	41.7	0.454	
$bb\bar{u}\bar{d}$	η_5	115	$7.0-9.0$	8.0	10.2 ± 0.3	42.8	0.215	10.60
	η_6	115	$7.0-9.2$	8.0	10.2 ± 0.3	42.0	0.304	
	η_7	115	$6.5-8.6$	7.6	10.2 ± 0.3	43.2	0.241	
	η_8	115	$6.8-8.8$	7.6	10.2 ± 0.3	41.7	0.343	
	η_1	125	$6.9-8.6$	7.6	10.7 ± 0.3	42.1	0.155	
	η_2	125	$6.9-8.8$	7.6	10.7 ± 0.4	44.5	0.170	
$bb\bar{q}\bar{s}$	η_3	120	$6.2-9.8$	8.0	10.4 ± 0.3	48.9	0.452	
	η_4	120	$6.5-9.8$	8.0	10.4 ± 0.3	49.3	0.446	10.69
	η_5	120	$6.6-9.8$	8.0	10.3 ± 0.3	52.3	0.298	
	η_6	120	$6.6-9.8$	8.0	10.3 ± 0.4	52.1	0.418	
	η_7	120	$6.2-9.6$	8.0	10.4 ± 0.3	48.1	0.342	
	η_8	120	$5.8-9.6$	8.0	10.4 ± 0.3	46.3	0.491	
$bb\bar{s}\bar{s}$	η_1	130	$7.0-9.7$	8.5	11.0 ± 0.3	40.8	0.336	
	η_2	130	$7.2-9.9$	8.5	10.9 ± 0.3	42.9	0.370	10.78
	η_3	120	$6.2-9.8$	8.0	10.4 ± 0.3	48.1	0.657	
	η_4	120	$6.2-9.8$	8.0	10.4 ± 0.3	48.5	0.651	

TABLE XIII: Numerical results for the doubly-charmed/bottomed $QQ\bar{q}\bar{q}$, $QQ\bar{u}\bar{d}$, $QQ\bar{q}\bar{s}$ and $QQ\bar{s}\bar{s}$ systems with $J^P=1^+$.

After performing the QCD sum rule analysis to the doubly-charmed/bottomed $QQ\bar{q}\bar{q}$, $QQ\bar{u}\bar{d}$, $QQ\bar{q}\bar{s}$ and $QQ\bar{s}\bar{s}$ systems with $J^P=0^-, 0^+, 1^-$ and 1^+, we collect the numerical results for all these tetraquark states in Tables X – XIII [55]. We take into account only the uncertainty of the values of the threshold parameter and variation of the Borel mass to obtain the errors. The other possible error sources, including the truncation of the OPE series, the uncertainty of the quark masses and the condensate values, are not considered. From these results, one finds that there are no stable sum rules for the 0^+ and 1^+ $cc\bar{q}\bar{q}$ and $cc\bar{u}\bar{d}$ systems, which implies that these tetraquark states probably do not exist. The corresponding $bb\bar{q}\bar{q}$ and $bb\bar{u}\bar{d}$ sum rules are relatively more stable.

We also give the open charm/bottom thresholds for all tetraquark states in Tabels X – XIII. One can easily find that the extracted masses of the $cc\bar{q}\bar{q}$, $cc\bar{q}\bar{s}$, and $cc\bar{s}\bar{s}$ doubly charmed states are above the $D^{(*)(+/0)}_{(0/1)}D^{(*)(+/0)}_{(0/1)}$, $D^{(*)+}_{(0/1)}D^{(*)+}_{s(0/1)}$, $D^{(*)+}_{s(0/1)}D^{(*)+}_{s(0/1)}$, and $\bar{N}\Omega_{cc}$ thresholds. They can decay into the two meson/baryon final states easily through the fall-apart mechanism. They are very broad resonances and difficult to be observed experimentally. However, the situations are very different for the doubly bottomed systems. In Tables X – XIII, the masses of the $bb\bar{q}\bar{q}$, $bb\bar{u}\bar{d}$, $bb\bar{q}\bar{s}$, and $bb\bar{s}\bar{s}$

are below the $\bar{B}^0\bar{B}^0, \bar{B}_s^0\bar{B}_s^0$ and $\bar{N}+\Omega_{bb}$ thresholds. In other words, the tetraquark states $bb\bar{q}\bar{q}$, $bb\bar{u}\bar{d}$, $bb\bar{q}\bar{s}$, and $bb\bar{s}\bar{s}$ are stable i.e, they only decay via electromagnetic and weak interactions. This observation is consistent with the conclusions in Refs. [54, 59, 66].

VI. MASS SPECTRUM OF THE OPEN-FLAVOR TETRAQUARK STATES

The $bc\bar{q}\bar{q}$ systems were studied in Refs. [64, 65, 110] and their mass predictions are below the thresholds of B^-D^+ and $\bar{B}^0D^0$. In Refs. [57, 111, 112], the authors studied the $c\bar{q}\bar{b}q$ systems and indicated that there may exist B_c-like molecular states. In this section we study the open-flavor $bc\bar{q}\bar{q}$, $bc\bar{s}\bar{s}$ and $qc\bar{q}\bar{b}$, $sc\bar{s}\bar{b}$ thetraquark systems with $J^P=0^+$ and 1^+ in QCD sum rules.

The QCD sum rules analyses are the same with the previous sections and we ignore the details here. We collect the numerical results for the scalar and axial-vector $bc\bar{q}\bar{q}, bc\bar{s}\bar{s}$ tetraquarks states in Tables XIV and XV while for $qc\bar{q}\bar{b}, qc\bar{s}\bar{b}$ tetraquarks states in Tables XVI and XVII, respectively [56]. From these results, we find that the $bc\bar{q}\bar{q}, bc\bar{s}\bar{s}$ tetraquark systems have much bigger pole contributions than the $qc\bar{q}\bar{b}, qc\bar{s}\bar{b}$ systems, which results in broader Borel windows for the previous systems. The mass sum rules for the $bc\bar{q}\bar{q}, bc\bar{s}\bar{s}$ systems are more stable.

The numerical results in Tables XIV–XVII show that the $bc\bar{q}\bar{q}$, $bc\bar{s}\bar{s}$ and $qc\bar{q}\bar{b}$, $sc\bar{s}\bar{b}$ tetraquark states lie below the open-flavor thresholds $D^{(*)}\bar{B}^{(*)}$, $D_s^{(*)}\bar{B}_s^{(*)}$ and $D^{(*)}B^{(*)}$, $D_s^{(*)}B_s^{(*)}$, respectively. They cannot decay into the open-flavor final states via the strong interaction due to the kinematic limits. But the $qc\bar{q}\bar{b}$ and $sc\bar{s}\bar{b}$ states can decay into B_c plus a light meson, such as $X(0^+)\to B_c\pi, B_c\eta$ and $X(1^+)\to B_c\rho, B_c\omega$. Such channels are suggested for the future search of these possible $qc\bar{q}\bar{b}$, $sc\bar{s}\bar{b}$ states. However, the $bc\bar{q}\bar{q}$ and $bc\bar{s}\bar{s}$ tetraquark states cannot decay through these fall-apart mechanisms, suggesting dominantly weak decay mechanisms.

System	Current	$s_0(\text{GeV}^2)$	$[M^2_{\text{min}},M^2_{\text{max}}](\text{GeV}^2)$	$m_X(\text{GeV})$	PC(%)
$bc\bar{q}\bar{q}$	J_1	60 ± 2	$5.4-6.2$	7.27 ± 0.19	35.5
	J_2	59 ± 2	$6.1-6.4$	7.16 ± 0.16	32.9
	J_3	58 ± 2	$5.4-6.0$	7.14 ± 0.16	33.9
	J_4	60 ± 2	$6.1-6.4$	7.23 ± 0.19	33.5
$bc\bar{s}\bar{s}$	J_1	61 ± 2	$4.9-6.4$	7.35 ± 0.17	39.1
	J_4	60 ± 2	$5.6-6.5$	7.26 ± 0.24	36.7

TABLE XIV: Numerical results for the $bc\bar{q}\bar{q}$ and $bc\bar{s}\bar{s}$ systems with $J^P=0^+$.

System	Current	$s_0(\text{GeV}^2)$	$[M^2_{\text{min}},M^2_{\text{max}}](\text{GeV}^2)$	m_X (GeV)	PC(%)
$bc\bar{q}\bar{q}$	$J_{1\mu}$	59 ± 2	$5.5-6.1$	7.21 ± 0.16	34.7
	$J_{2\mu}$	60 ± 2	$5.3-6.2$	7.27 ± 0.20	37.5
	$J_{3\mu}$	60 ± 2	$5.4-6.3$	7.26 ± 0.19	36.8
	$J_{4\mu}$	58 ± 2	$5.3-6.0$	7.13 ± 0.17	35.7
$bc\bar{s}\bar{s}$	$J_{2\mu}$	61 ± 2	$4.9-6.4$	7.35 ± 0.22	41.2
	$J_{3\mu}$	61 ± 2	$4.9-6.4$	7.34 ± 0.22	42.1

TABLE XV: Numerical results for the $bc\bar{q}\bar{q}$ and $bc\bar{s}\bar{s}$ systems with $J^P=1^+$.

System	Current	$s_0(\text{GeV}^2)$	$[M^2_{\text{min}},M^2_{\text{max}}](\text{GeV}^2)$	$m_X(\text{GeV})$	PC(%)
$qc\bar{q}\bar{b}$	J_1	55 ± 2	$7.8-8.0$	7.11 ± 0.15	10.2
$sc\bar{s}\bar{b}$	J_1	56 ± 2	$6.6-8.1$	7.16 ± 0.18	14.4
	J_2	56 ± 2	$8.8-9.2$	7.10 ± 0.26	10.6
	J_4	56 ± 2	$8.8-9.1$	7.10 ± 0.27	10.9

TABLE XVI: Numerical results for the $qc\bar{q}\bar{b}$ and $sc\bar{s}\bar{b}$ systems with $J^P=0^+$.

System	Current	$s_0(\mathrm{GeV}^2)$	$[M^2_{\rm min},M^2_{\rm max}](\mathrm{GeV}^2)$	$m_X(\mathrm{GeV})$	PC(%)
$qc\bar{q}\bar{b}$	$J_{1\mu}$	55 ± 2	$7.9-8.2$	7.10 ± 0.16	10.4
	$J_{2\mu}$	55 ± 2	$7.9-8.2$	7.09 ± 0.16	10.7
$sc\bar{s}\bar{b}$	$J_{1\mu}$	55 ± 2	$6.7-7.9$	7.11 ± 0.16	14.0
	$J_{2\mu}$	56 ± 2	$6.7-8.3$	7.15 ± 0.20	14.2
	$J_{3\mu}$	52 ± 2	$6.7-7.3$	6.90 ± 0.14	11.6
	$J_{4\mu}$	52 ± 2	$6.7-7.3$	6.92 ± 0.18	11.0

TABLE XVII: Numerical results for the $qc\bar{q}\bar{b}$ and $sc\bar{s}\bar{b}$ systems with $J^P=1^+$.

VII. MASS SPECTRUM OF THE QUARKONIUM HYBRID $\bar{Q}GQ$ STATES

Including only dimension four condensate in the correlation functions, the charmonium hybrids with $J^{PC}=0^{-+},0^{+-},1^{-+},1^{--}$ and 2^{-+} were unstable in Refs. [30–32]. To stabilize these hybrid sum rules, we reinvestigated the two-point correlation functions and considered also dimension six tri-gluon condensate [37].

As shown in Fig. 5, the gluon condensate is the dominant power correction to the charmonium hybrid sum rule in Eq. (12). However, the tri-gluon condensate is too large to be neglected. By studying the OPE convergence and the pole contribution, we obtain the suitable working region of the Borel mass 4.6 $\mathrm{GeV}^2\leq M_B^2\leq 6.5$ GeV^2 with the continuum threshold $s_0=17$ GeV^2. In Fig. 6, the Borel curves are very stable in the the regions of these parameters. We then extracted the mass of the 1^{-+} charmonium hybrid as [37]

$$m_X=(3.70\pm0.21)\mathrm{GeV}, \tag{36}$$

which is about 0.5 GeV lower than the lattice result in Ref. [45]. One finds that the tri-gluon condensate can stabilize the hybrid sum rules and lead to the reliable mass prediction. After performing the sum rule analysis for all channels, we collect the numerical results for the charmonium and bottomonium hybrids in Tables XVIII and XIX respectively [37]. Only errors from the uncertainties in the charm quark mass and the condensates are taken into account. We do not consider other possible error sources such as truncation of the OPE series, the uncertainty of the threshold value s_0 and the variation of Borel mass M_B.

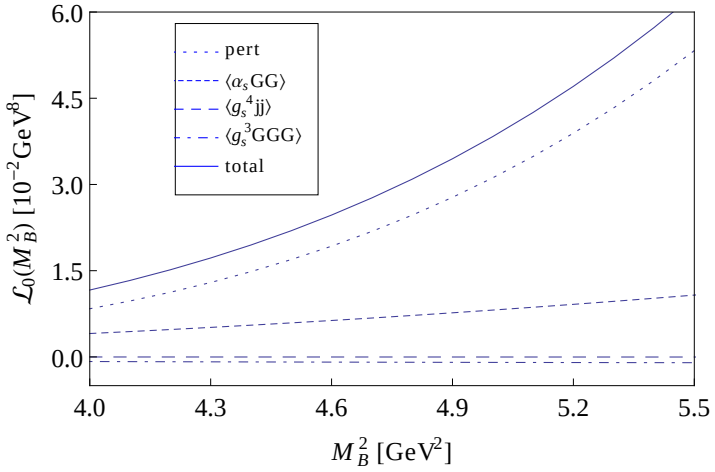

FIG. 5: OPE convergence for the 1^{-+} charmonium hybrid.

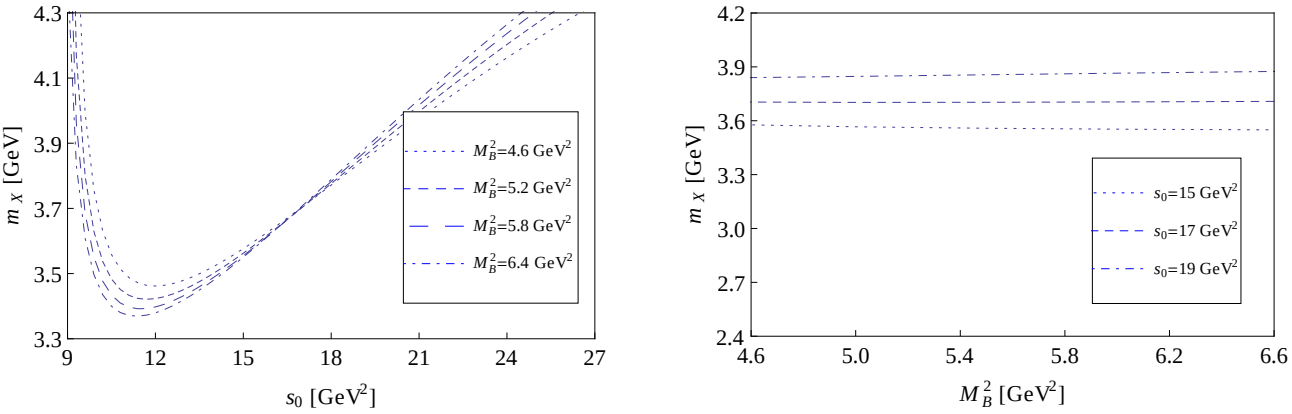

FIG. 6: Variations of m_X with s_0 and M_B^2 for the $J^{PC}=1^{-+}$ charmonium hybrid.

J^{PC}	$s_0(\mathrm{GeV}^2)$	$[M^2_{\mathrm{min}},M^2_{\mathrm{max}}](\mathrm{GeV}^2)$	$m_X(\mathrm{GeV})$	PC(%)
1^{--}	15	$2.5-4.8$	3.36 ± 0.15	18.3
0^{-+}	16	$5.6-7.0$	3.61 ± 0.21	15.4
1^{-+}	17	$4.6-6.5$	3.70 ± 0.21	18.8
2^{-+}	18	$3.9-7.2$	4.04 ± 0.23	26.0
0^{+-}	20	$6.0-7.4$	4.09 ± 0.23	15.5
2^{++}	23	$3.9-7.5$	4.45 ± 0.27	21.5
1^{+-}	24	$2.5-8.4$	4.53 ± 0.23	33.2
1^{++}	30	$4.6-11.4$	5.06 ± 0.44	30.4
0^{++}	34	$5.6-14.6$	5.34 ± 0.45	36.3
0^{--}	35	$6.0-12.3$	5.51 ± 0.50	31.0

TABLE XVIII: Mass spectrum of the charmonium hybrid states.

J^{PC}	$s_0(\mathrm{GeV}^2)$	$[M^2_{\mathrm{min}},M^2_{\mathrm{max}}](\mathrm{GeV}^2)$	$m_X(\mathrm{GeV})$	PC(%)
1^{--}	105	$11-17$	9.70 ± 0.12	17.2
0^{-+}	104	$14-16$	9.68 ± 0.29	17.3
1^{-+}	107	$13-19$	9.79 ± 0.22	20.4
2^{-+}	105	$12-19$	9.93 ± 0.21	21.7
0^{+-}	114	$14-19$	10.17 ± 0.22	17.6
2^{++}	120	$12-20$	10.64 ± 0.33	19.7
1^{+-}	123	$10-21$	10.70 ± 0.53	28.5
1^{++}	134	$13-27$	11.09 ± 0.60	27.7
0^{++}	137	$13-31$	11.20 ± 0.48	30.0
0^{--}	142	$14-25$	11.48 ± 0.75	24.1

TABLE XIX: Mass spectrum of the bottomonium hybrid states.

$Y(4260)$ was first observed in the $J/\psi\pi^+\pi^-$ channel by Barbar collaboration [119] and confirmed by CLEO [120] and Belle [121] collaborations. Its quantum number is $J^{PC}=1^{--}$. The open charm decay mode $Y(4260)\to D\bar{D}$ has not been observed in spite of the large phase space. This is consistent with the expectation of the hybrid meson decay pattern, which disfavors the two S-wave meson final states but prefers the $S+P$ decay mode. Since its discovery, $Y(4260)$ was considered as a good candidate of the charmonium hybrid [122–124]. However, the mass of the 1^{--}

channel of charmonium hybrid in Table XVIII is about 3.36 ± 0.15 GeV, which is much lower than the mass of $Y(4260)$ meson.

In the MIT bag model [4, 5], the hybrid states with $J^{PC}=(0,1,2)^{-+},1^{--}$ were considered to be composed of a S-wave color-octet $q\bar{q}$ pair and an excited gluon field with $J_g^{P_gC_g}=1^{+-}$. This supermultiplet was confirmed in lattice QCD [45] and the P-wave quasi gluon approach [125] for the heavy quarkonium hybrid systems, in which a heavier hybrid supermultiplet was also predicted including states with $J^{PC}=0^{+-},(1^{+-})^3,(2^{+-})^2,3^{+-},(0,1,2)^{++}$. In Tables XVIII and XVIII, our results support such supermultiplet structures that the hybrid states with $J^{PC}=(0,1,2)^{-+},1^{--}$ form the lowest supermultiplet while those with the quantum numbers $J^{PC}=0^{+-},2^{++},1^{+-},1^{++},0^{++}$ form a heavier supermultiplet. The hybrid with $J^{PC}=0^{--}$ is the heaviest one, which may suggest that this state has a higher gluonic excitation.

The numerical results of the $\bar{b}gc$ hybrid states are collected in Table XX [38]. In the $\bar{b}Gc$ hybrid systems, the supermultiplet structures are still present. In Table XX, the hybrid states with $J^P=(0,1,2)^-,1^-$ form the lightest supermultiplet while a heavier one is formed by the states with $J^P=(0^+)^2,(1^+)^2,2^+$. We obtain two vector states with $J^P=1^-$ in the lightest hybrid supermultiplet while two 1^+ two 0^+ hybrids in the heavier supermultiplet. The mass differences for the vector, axial-vector and scalar doublet are 0.12 GeV, 0.53 GeV and 1.18 GeV, respectively. There also exists a pseudoscalar doublet with the mass difference around 1.58 GeV. The existence of these hybrid doublets suggests that the operators are separately probing a ground and excited state. The two hybrids with the same quantum numbers have very different gluonic excitations.

Operator	J^P	$s_0(\text{GeV}^2)$	$[M^2_{\text{min}},M^2_{\text{max}}](\text{GeV}^2)$	$m_X(\text{GeV})$	PC(%)
$\tilde{J}^{(2)}_\mu$	1^-	52	$5.90-6.50$	6.83 ± 0.16	55.9
$\tilde{J}^{(1)}_\mu$	0^-	61	$10.4-11.5$	6.90 ± 0.22	23.4
$J^{(1)}_\mu$	1^-	62	$9.00-10.7$	6.95 ± 0.22	26.1
$J^{(3)}_{\mu\nu}$	2^-	59	$8.00-10.5$	7.15 ± 0.22	29.4
$\tilde{J}^{(2)}_\mu$	0^+	69	$10.9-12.0$	7.37 ± 0.31	22.8
$\tilde{J}^{(3)}_{\mu\nu}$	2^+	66	$8.00-11.2$	7.67 ± 0.18	39.8
$J^{(2)}_\mu$	1^+	71	$5.90-8.00$	7.77 ± 0.24	59.4
$\tilde{J}^{(1)}_\mu$	1^+	77	$9.00-10.0$	8.28 ± 0.38	54.3
$J^{(1)}_\mu$	0^+	84	$10.4-12.2$	8.55 ± 0.44	55.7
$J^{(2)}_\mu$	0^-	76	$10.9-14.2$	8.48 ± 0.67	24.4

TABLE XX: Numerical results of the $\bar{b}gc$ hybrid states.

VIII. SUMMARY

In this article, we have reviewed our previous investigations of the quarkoniumlike tetraquark $qQ\bar{q}\bar{Q}$ systems [51, 52], doubly charmed/bottomed tetraquark $QQ\bar{q}\bar{q}$ systems [55], open-flavor $bc\bar{q}\bar{q}$ and $qc\bar{q}\bar{b}$ systems [56], heavy quarkonium hybrid $\bar{Q}GQ$ systems [37] and the bottom-charm hybrid $\bar{b}Gc$ systems [38] in the QCD sum rules approach.

The discovery of the XYZ states is a significant challenge to our understanding of the QCD hadronic spectrum. To understand the nature of these new mesons, the formalism of QCD sum rules provides is very useful. We have evaluated the mass spectra of the heavy tetraquarks and the quarkonium hybrids in the framework of QCD sum rules. The study of the charmoniumlike tetraquark state $qc\bar{q}\bar{c}$ provides possible interpretations for several new XYZ states, such as $Y(4660),X(3872),Z_c(3900)$ and $Z_c(4025)$. The extracted mass of the 1^{--} $qc\bar{q}\bar{c}$ tetraquark state is about $m_X=(4.64\pm0.09)$ GeV, which is consistent with the mass of $Y(4660)$ meson and may indicate a possible tetraquark interpretation. The mass of 1^{++} channel is about $m_X=(4.03\pm0.11)$ GeV, which is slightly above the mass of $X(3872)$. Considering the uncertainties, the tetraquark interpretation of $X(3872)$ is not excluded. The calculations of the 1^{++} and 1^{+-} $qc\bar{q}\bar{c}$ channels lead to the lowest lying ground states around 3.9–4.2 GeV, which may support the charged states $Z_c(3900)$ and $Z_c(4025)$ as the candidate of the isovector charmoniumlike tetraquark states with $J^P=1^+$. Surprisingly, the mass spectrum of the charmonium hybrid states in Table XVIII is much lower than that obtained in lattice QCD [45]. For non-exotic J^{PC}, the effect of mixing with quarkonium states may raise these mass predictions [108].

All the $bb\bar{q}\bar{q}$, $bb\bar{u}\bar{d}$, $bb\bar{q}\bar{s}$, $bb\bar{s}\bar{s}$, $bc\bar{q}\bar{q}$ and $bc\bar{s}\bar{s}$ tetraquark states lie below the $\bar{B}^0\bar{B}^0,\bar{B}^0_s\bar{B}^0_s$, $\bar{N}+\Omega_{bb}$, $D^{(*)}\bar{B}^{(*)}$ and $D^{(*)}_s\bar{B}^{(*)}_s$ thresholds. These tetraquark states cannot decay via strong interaction into both the two meson and two

baryon final states. They should be very narrow because they can decay via electromagnetic and weak interactions only. These states may be searched for at LHCb and RHIC in the future, where many heavy quarks are produced.

ACKNOWLEDGMENTS

This project was supported by the the National Natural Science Foundation of China under Grant NO. 11261130311 and the Natural Sciences and Engineering Research Council of Canada (NSERC).

[1] S. Godfrey and N. Isgur, Phys.Rev. **D32**, 189 (1985).
[2] J. Beringer et al. (Particle Data Group), Phys.Rev. **D86**, 010001 (2012).
[3] R. Jaffe and K. Johnson, Phys.Lett. **B60**, 201 (1976).
[4] T. Barnes, F. Close, F. de Viron, and J. Weyers, Nucl.Phys. **B224**, 241 (1983).
[5] M. S. Chanowitz and S. R. Sharpe, Nucl. Phys. **B222**, 211 (1983).
[6] N. Isgur, R. Kokoski, and J. E. Paton, Phys.Rev.Lett. **54**, 869 (1985).
[7] F. E. Close and P. R. Page, Phys.Rev. **D52**, 1706 (1995).
[8] T. Barnes, F. E. Close, and E. S. Swanson, Phys. Rev. **D52**, 5242 (1995).
[9] P. R. Page, E. S. Swanson, and A. P. Szczepaniak, Phys. Rev. **D59**, 034016 (1999).
[10] F. E. Close and P. R. Page, Nucl.Phys. **B443**, 233 (1995).
[11] C. McNeile, C. W. Bernard, T. A. DeGrand, C. E. DeTar, S. A. Gottlieb, et al., Nucl.Phys.Proc.Suppl. **73**, 264 (1999).
[12] P. Lacock and K. Schilling (TXL), Nucl. Phys. Proc. Suppl. **73**, 261 (1999), hep-lat/9809022.
[13] C. Bernard, T. Burch, E. Gregory, D. Toussaint, C. E. DeTar, et al., Phys.Rev. **D68**, 074505 (2003), hep-lat/0301024.
[14] J. Hedditch, W. Kamleh, B. Lasscock, D. Leinweber, A. Williams, et al., Phys.Rev. **D72**, 114507 (2005), hep-lat/0509106.
[15] J. Govaerts, F. de Viron, D. Gusbin, and J. Weyers, Phys.Lett. **B128**, 262 (1983).
[16] J. Govaerts, F. de Viron, D. Gusbin, and J. Weyers, Nucl. Phys. **B248**, 1 (1984).
[17] J. Latorre, S. Narison, P. Pascual, and R. Tarrach, Phys.Lett. **B147**, 169 (1984).
[18] J. I. Latorre, P. Pascual, and S. Narison, Z. Phys. **C34**, 347 (1987).
[19] I. Balitsky, D. Diakonov, and A. Yung, Z.Phys. **C33**, 265 (1986).
[20] H. Jin, J. Korner, and T. G. Steele, Phys.Rev. **D67**, 014025 (2003), hep-ph/0211304.
[21] K. G. Chetyrkin and S. Narison, Phys.Lett. **B485**, 145 (2000), hep-ph/0003151.
[22] S.-L. Zhu, Phys.Rev. **D60**, 097502 (1999), hep-ph/9903537.
[23] D. Thompson et al. (E852 Collaboration), Phys.Rev.Lett. **79**, 1630 (1997), hep-ex/9705011.
[24] A. Abele et al. (Crystal Barrel), Phys. Lett. **B423**, 175 (1998).
[25] A. Abele et al. (Crystal Barrel), Phys. Lett. **B446**, 349 (1999).
[26] G. S. Adams et al. (E862), Phys. Lett. **B657**, 27 (2007), hep-ex/0612062.
[27] E. Klempt and A. Zaitsev, Phys. Rept. **454**, 1 (2007), hep-ph/0708.4016.
[28] B. Ketzer, PoS **QNP2012**, 025 (2012), hep-ex/1208.5125.
[29] D. Horn and J. Mandula, Phys.Rev. **D17**, 898 (1978).
[30] J. Govaerts, L. J. Reinders, H. R. Rubinstein, and J. Weyers, Nucl. Phys. **B258**, 215 (1985).
[31] J. Govaerts, L. J. Reinders, and J. Weyers, Nucl. Phys. **B262**, 575 (1985).
[32] J. Govaerts, L. J. Reinders, P. Francken, X. Gonze, and J. Weyers, Nucl. Phys. **B284**, 674 (1987).
[33] S.-L. Zhu, Phys. Rev. **D60**, 031501 (1999), hep-ph/9812469.
[34] C.-F. Qiao, L. Tang, G. Hao, and X.-Q. Li, J.Phys. **G39**, 015005 (2012), 1012.2614.
[35] D. Harnett, R. Kleiv, T. Steele, and H.-y. Jin, J.Phys. **G39**, 125003 (2012).
[36] R. Berg, D. Harnett, R. Kleiv, and T. Steele, Phys.Rev. **D86**, 034002 (2012).
[37] W. Chen, R. Kleiv, T. Steele, B. Bulthuis, D. Harnett, et al., JHEP **09**, 019 (2013).
[38] W. Chen, T. Steele, and S.-L. Zhu, J.Phys. **G41**, 025003 (2014).
[39] G. Chiladze, A. F. Falk, and A. A. Petrov, Phys.Rev. **D58**, 034013 (1998), hep-ph/9804248.
[40] S. Perantonis and C. Michael, Nucl.Phys. **B347**, 854 (1990).
[41] K. J. Juge, J. Kuti, and C. J. Morningstar, Phys. Rev. Lett. **82**, 4400 (1999), hep-ph/9902336.
[42] Y. Liu and X.-Q. Luo, Phys.Rev. **D73**, 054510 (2006), hep-lat/0511015.
[43] X.-Q. Luo and Y. Liu, Phys.Rev. **D74**, 034502 (2006), hep-lat/0512044.
[44] L. Liu, S. M. Ryan, M. Peardon, G. Moir, and P. Vilaseca, PoS **LATTICE2011**, 140 (2011), 1112.1358.
[45] L. Liu et al. (Hadron Spectrum Collaboration), JHEP **1207**, 126 (2012).
[46] H.-X. Chen, A. Hosaka, and S.-L. Zhu, Phys. Lett. **B650**, 369 (2007).
[47] H.-X. Chen, A. Hosaka, and S.-L. Zhu, Phys. Rev. **D76**, 094025 (2007).
[48] R. D. Matheus, S. Narison, M. Nielsen, and J. M. Richard, Phys. Rev. **D75**, 014005 (2007), hep-ph/0608297.
[49] L. Maiani, A. D. Polosa, and V. Riquer, Phys. Rev. Lett. **99**, 182003 (2007).
[50] D. Ebert, R. N. Faustov, and V. O. Galkin, Phys. Lett. **B634**, 214 (2006), hep-ph/0512230.
[51] W. Chen and S.-L. Zhu, Phys. Rev. **D83**, 034010 (2011).

[52] W. Chen and S.-L. Zhu, Phys. Rev. **D81**, 105018 (2010).
[53] M.-L. Du, W. Chen, X.-L. Chen, and S.-L. Zhu, Chin.Phys. **C37**, 033104 (2013).
[54] J. Carlson, L. Heller, and J. Tjon, Phys.Rev. **D37**, 744 (1988).
[55] M.-L. Du, W. Chen, X.-L. Chen, and S.-L. Zhu, Phys.Rev. **D87**, 014003 (2013).
[56] W. Chen, T. Steele, and S.-L. Zhu (2013).
[57] R. M. Albuquerque, X. Liu, and M. Nielsen, Phys.Lett. **B718**, 492 (2012).
[58] F. S. Navarra, M. Nielsen, and S. H. Lee, Phys.Lett. **B649**, 166 (2007), hep-ph/0703071.
[59] M. Zhang, H. Zhang, and Z. Zhang, Commun.Theor.Phys. **50**, 437 (2008).
[60] S. Pepin, F. Stancu, M. Genovese, and J. Richard, Phys.Lett. **B393**, 119 (1997), hep-ph/9609348.
[61] J. Vijande, A. Valcarce, and K. Tsushima, Phys.Rev. **D74**, 054018 (2006), hep-ph/0608316.
[62] J. Vijande, A. Valcarce, and N. Barnea, Phys.Rev. **D79**, 074010 (2009).
[63] D. Brink and F. Stancu, Phys.Rev. **D57**, 6778 (1998).
[64] B. Silvestre-Brac and C. Semay, Z.Phys. **C59**, 457 (1993).
[65] S. Zouzou, B. Silvestre-Brac, C. Gignoux, and J. Richard, Z.Phys. **C30**, 457 (1986).
[66] A. V. Manohar and M. B. Wise, Nucl.Phys. **B399**, 17 (1993), hep-ph/9212236.
[67] Y. Cui, X.-L. Chen, W.-Z. Deng, and S.-L. Zhu, High Energy Phys. Nucl. Phys. **31**, 7 (2007), hep-ph/0607226.
[68] B. A. Gelman and S. Nussinov, Phys.Lett. **B551**, 296 (2003), hep-ph/0209095.
[69] M. A. Moinester, Z.Phys. **A355**, 349 (1996), hep-ph/9506405.
[70] M. Bander and A. Subbaraman, Phys.Rev. **D50**, R5478 (1994), hep-ph/9407309.
[71] J. Ader, J. Richard, and P. Taxil, Phys.Rev. **D25**, 2370 (1982).
[72] J. M. Richard, Nucl.Phys.Proc.Suppl. **21**, 254 (1991).
[73] H. J. Lipkin, Phys.Lett. **B172**, 242 (1986).
[74] H. Lipkin, Phys.Lett. **B45**, 267 (1973).
[75] T. Carames, A. Valcarce, and J. Vijande, Phys.Lett. **B699**, 291 (2011).
[76] G. T. Bodwin, E. Braaten, E. Eichten, S. L. Olsen, T. K. Pedlar, et al. (2013), hep-ph/1307.7425.
[77] M. A. Shifman, A. I. Vainshtein, and V. I. Zakharov, Nucl. Phys. **B147**, 385 (1979).
[78] L. J. Reinders, H. Rubinstein, and S. Yazaki, Phys. Rept. **127**, 1 (1985).
[79] P. Colangelo and A. Khodjamirian, Frontier of Particle Physics **3** (2000), hep-ph/0010175.
[80] M. Nielsen, F. S. Navarra, and S. H. Lee, Phys. Rept. **497**, 41 (2010).
[81] K. G. Wilson, Phys. Rev. **179**, 1499 (1969).
[82] K.-C. Yang, W. Y. P. Hwang, E. M. Henley, and L. S. Kisslinger, Phys. Rev. **D47**, 3001 (1993).
[83] S. Narison, Phys.Lett. **B707**, 259 (2012).
[84] S. Narison, Phys.Lett. **B693**, 559 (2010).
[85] J. H. Kuhn, M. Steinhauser, and C. Sturm, Nucl.Phys. **B778**, 192 (2007), hep-ph/0702103.
[86] K. G. Chetyrkin et al., Phys. Rev. **D80**, 074010 (2009).
[87] E. Bagan, J. Latorre, P. Pascual, and R. Tarrach, Nucl.Phys. **B254**, 555 (1985).
[88] S. C. Generalis and D. J. Broadhurst, Phys. Lett. **B139**, 85 (1984).
[89] H.-X. Chen, A. Hosaka, and S.-L. Zhu, Phys. Rev. **D78**, 054017 (2008).
[90] C.-K. Jiao, W. Chen, H.-X. Chen, and S.-L. Zhu, Phys. Rev. **D79**, 114034 (2009).
[91] X. L. Wang et al. (Belle), Phys. Rev. Lett. **99**, 142002 (2007).
[92] F.-K. Guo, C. Hanhart, and U.-G. Meissner, Phys. Lett. **B665**, 26 (2008).
[93] C.-F. Qiao, J. Phys. **G35**, 075008 (2008).
[94] G.-J. Ding, J.-J. Zhu, and M.-L. Yan, Phys.Rev. **D77**, 014033 (2008).
[95] D. Ebert, R. N. Faustov, and V. O. Galkin, Eur. Phys. J. **C58**, 399 (2008).
[96] R. M. Albuquerque and M. Nielsen, Nucl. Phys. **A815**, 53 (2009).
[97] S. K. Choi et al. (Belle), Phys. Rev. Lett. **91**, 262001 (2003).
[98] R. Aaij et al. (LHCb), Phys.Rev.Lett. **110**, 222001 (2013).
[99] X. Liu, Z.-G. Luo, Y.-R. Liu, and S.-L. Zhu, Eur. Phys. J. **C61**, 411 (2009).
[100] Y.-R. Liu, X. Liu, W.-Z. Deng, and S.-L. Zhu, Eur. Phys. J. **C56**, 63 (2008).
[101] E. S. Swanson, Phys. Lett. **B598**, 197 (2004), hep-ph/0406080.
[102] E. S. Swanson, Phys. Lett. **B588**, 189 (2004), hep-ph/0311229.
[103] F. E. Close and P. R. Page, Phys. Lett. **B578**, 119 (2004), hep-ph/0309253.
[104] C. E. Thomas and F. E. Close, Phys. Rev. **D78**, 034007 (2008).
[105] T. Fernandez-Carames, A. Valcarce, and J. Vijande, Phys. Rev. Lett. **103**, 222001 (2009).
[106] D. V. Bugg, Phys. Lett. **B598**, 8 (2004), hep-ph/0406293.
[107] F. E. Close and S. Godfrey, Phys. Lett. **B574**, 210 (2003), hep-ph/0305285.
[108] W. Chen, H.-y. Jin, R. Kleiv, T. Steele, M. Wang, et al., Phys.Rev. **D88**, 045027 (2013).
[109] R. D. Matheus, F. Navarra, M. Nielsen, and C. Zanetti, Phys.Rev. **D80**, 056002 (2009).
[110] G. Q. Feng, X. H. Guo, and B. S. Zou (2013), hep-ph/1309.7813.
[111] J.-R. Zhang and M.-Q. Huang, Phys. Rev. **D80**, 056004 (2009).
[112] Z.-F. Sun, X. Liu, M. Nielsen, and S.-L. Zhu, Phys.Rev. **D85**, 094008 (2012).
[113] M. Ablikim et al. (BESIII Collaboration) (2013), hep-ex/1308.2760.
[114] W. Chen, T. Steele, M.-L. Du, and S.-L. Zhu, Eur.Phys.J. **C74**, 2773 (2014).
[115] J. He, X. Liu, Z.-F. Sun, and S.-L. Zhu, Eur.Phys.J. **C73**, 2635 (2013).

[116] X. Wang, Y. Sun, D.-Y. Chen, X. Liu, and T. Matsuki, Eur.Phys.J. **C74**, 2761 (2014).
[117] C.-Y. Cui, Y.-L. Liu, and M.-Q. Huang (2013), hep-ph/1308.3625.
[118] C.-F. Qiao and L. Tang (2013), hep-ph/1308.3439.
[119] B. Aubert et al. (BABAR), Phys. Rev. Lett. **95**, 142001 (2005), hep-ex/0506081.
[120] Q. He et al. (CLEO), Phys. Rev. **D74**, 091104 (2006), hep-ex/0611021.
[121] C. Z. Yuan et al. (Belle), Phys. Rev. Lett. **99**, 182004 (2007).
[122] S.-L. Zhu, Phys. Lett. **B625**, 212 (2005), hep-ph/0507025.
[123] E. Kou and O. Pene, Phys. Lett. **B631**, 164 (2005), hep-ph/0507119.
[124] F. E. Close and P. R. Page, Phys. Lett. **B628**, 215 (2005), hep-ph/0507199.
[125] P. Guo, A. P. Szczepaniak, G. Galata, A. Vassallo, and E. Santopinto, Phys.Rev. **D78**, 056003 (2008).